CH9700124

Electromagnetic Properties of Neutrinos

F. Ould-Saada [1]
Physics Institute, University of Zurich

Abstract

Electromagnetic properties of neutrinos and their implications are discussed, and the experimental situation summarised. Spin precession in solar magnetic fields presents a solution of the solar neutrino problem. A magnetic moment, μ_ν, of the order of $10^{-11}\mu_B$ would be needed. In the simplest extension of the standard model, with non-vanishing neutrino masses, dipole moment interactions are allowed through higher order processes. A neutrino mass of $\sim 10\ eV$ would give $\mu_\nu \sim 10^{-18}\mu_B$, much smaller than the present experimental upper limit of $2 \times 10^{-10}\mu_B$. Although model-dependent, upper bounds on dipole moments from astrophysics and cosmology are 10 to 100 times more stringent. Any values of μ_ν, larger than the SM predictions, would then signal the onset of new physics. Among the processes sensitive to the magnetic moment, νe^- scattering presents two advantages: it is a pure weak, theoretically well understood process, and the recoil electron can be easily measured. A hypothetical electromagnetic contribution to the cross-section would dominate at low energies. A low background detector, MUNU, being built at the Bugey nuclear reactor is presented. It is based on a gas TPC, surrounded by a liquid scintillator. The threshold on the electron recoil energy can be set very low, around 500 keV, giving the experiment a good sensitivity to the magnetic moment of the $\overline{\nu_e}$, extending down to $2 \times 10^{-11}\mu_B$.

1 Introduction and Motivations

1.1 What do we know about neutrinos?

The neutrino, a neutral particle of spin one half, was proposed in 1930 by W. Pauli "...as a desperate remedy to save the principle of energy conservation in β-Decay...". The electron antineutrino, $\overline{\nu}_e$, was discovered a quarter of a century later by Reines and his collaborators[1, 2] at a nuclear reactor. The neutrino helicity was measured to be negative 1957[3]. The proof for the existence of a second Neutrino related to the muon was obtained in 1962[4] using high energy neutrinos produced by an accelerator. The existence of a third neutrino, ν_τ, related to the tau-lepton was inferred in 1975[5].

What do we know about neutrinos today? Neutrinos are weakly interacting, spin $\frac{1}{2}$ particles. There are 3 kinds of light neutrinos ν_e, ν_μ and ν_τ corresponding to the three known leptons e^-, μ^- and τ^- ($m_{\nu_i} > 45\ GeV/c^2$ from LEP data). Neutrinos are described in the framework of the standard model of electroweak interactions based on the group $SU(2)_L \times U(1)$. In the standard model neutrinos are massless and of Dirac type. Only ν_L and $\overline{\nu}_R$ have the weak interaction. ν_R and $\overline{\nu}_L$ are sterile. Up to now neutrinos are massless with the upper limits $m_{\nu_e} < 4.35\ eV/c^2$[6], $m_{\nu_\mu} < 170\ keV/c^2$[7], and $m_{\nu_\tau} < 24\ MeV/c^2$[8].

What needs to be learned about neutrinos today? Do they have a mass? If yes, why are they so much lighter than other leptons and quarks? (see-saw mechanism?) Do they oscillate in vacuum? in matter? What is the origin of the 'solar neutrino problem'? What is the origin of the 'atmospheric neutrino problem'? Are neutrinos heavy enough to explain dark matter? Are neutrinos Majorana (neutrinoless double β decay?) or Dirac particles? Do neutrinos interact electromagnetically? Do they acquire any dipole moment (magnetic or electric)? Do they have any structure (charge radius)?

1.2 Electromagnetic properties of neutrinos

Although neutrinos are neutral[9] ($Q_\nu < 2 \times 10^{-15}$), they can couple to the electromagnetic field through higher order weak interactions. The EM ν-Vertex (Fig.1) has the form

$$F_R(q^2, r_\nu^2)\gamma^\alpha - \left(\mu_{ll'} + d_{ll'}\gamma^5\right)\sigma^{\alpha\beta}q^\beta$$

The formfactor $F_R(q^2, r_\nu^2)$ is related to the charge radius r_ν: $F_R(q^2, r_\nu^2) \sim \frac{1}{6}q^2 r_\nu^2$. $\mu_{ll'}$ and $d_{ll'}$ are the magnetic and electric dipole moments, respectively.

For $l = l'$ one has a diagonal dipole moment ($\nu_{eL} \to \nu_{eR}$). In case $l \neq l'$ ($\nu_{eL} \to \nu_{\mu R}$), the neutrino is said to have a transition moment. For diagonal moments ($l = l'$) the dipole

[1] E-Mail: Farid.Ould-Saada@cern.ch

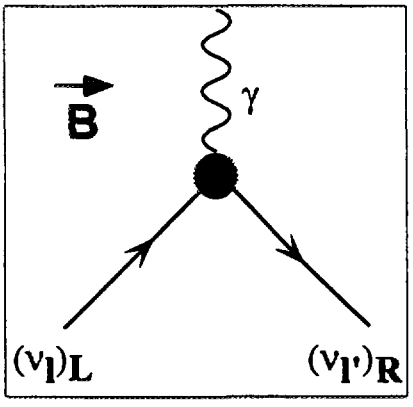

Figure 1: *Spin Precession in a magnetic field B.*

interaction energy has the known form: $\mu_\nu\langle\vec{s}\cdot\vec{B}\rangle$; $d_\nu\langle\vec{s}\cdot\vec{E}\rangle$. For highly relativitic neutrinos it is not possible to distinguish between the electric and magnetic dipole moments. What is measured experimentally is the recoil e^-, for example, not the neutrino. One thus defines an effective dipole moment (magnetic moment) ν_l as

$$\mu_{\nu_l} = \sqrt{\sum_{l'=e,\mu,\tau} \mid \mu_{ll'} - d_{ll'} \mid^2}$$

There exist two possible ways to describe neutrinos. A massive Dirac neutrino ν^D, for which $\nu \neq \overline{\nu}$, has four distinct states, whereas a Majorana neutrino ν^M[10], ($\nu = \overline{\nu}$) has 2 distinct states:

$$\nu^D = \begin{pmatrix} \nu_L \\ \overline{\nu}_L \\ \nu_R \\ \overline{\nu}_R \end{pmatrix} \; ; \; \nu^M = \begin{pmatrix} \nu_L \\ \nu_R \end{pmatrix}$$

If the neutrino is massless there is no way to distinguish between ν^D and ν^M. Dirac neutrinos may have a magnetic dipole moment, and if CP is not conserved, an electric dipole moment. For a Majorana neutrino the diagonal terms must vanish, as a consequence of CPT [12, 11].

In the standard model, including right handed (massive) neutrinos, Dirac neutrinos acquire a magnetic moment proportional to mass m_ν: $\mu_\nu \sim 3.2 \cdot 10^{-19}\frac{m_\nu}{eV} \cdot \mu_B$, where $\mu_B = e/2m_e$ is the Bohr Magneton. For a neutrino mass corresponding to the actual measured upper limit, $m_{\nu_e} \simeq 10\ eV$ one expects $\mu_\nu^{SM} \sim 3 \cdot 10^{-18}\mu_B$, whereas the laboratory limits are $\sim 10^{-10}\mu_B$. Therefore, a measurement of the magnetic moment of the neutrino probes new physics beyond the standard model.

1.3 The Solar Neutrino Problem

The comparison of the detected solar neutrino flux to the predictions of the solar models shows a clear deficit (Tab.1 and Fig.2), known as the Solar Neutrino Problem (SNP). Furthermore

Experiment	Process	E_ν^{thresh} [keV]	Sensitivity	data [SNU]	B-P [SNU]	T-C-L [SNU]
Homestake	$e - {}^{37}Cl \rightarrow \nu_e {}^{37}Ar$	0.814	${}^8B, Be$	$2.54 \pm 0.14 \pm 0.14$	8.0 ± 3.0	6.4
Kamiokande	$\nu e - \rightarrow \nu_e e -$	7.500	${}^8B$	$2.80^{\pm}0.19 \pm 0.33$	5.7 ± 2.4	4.4
Gallex	$e - {}^{71}Ga \rightarrow \nu_e {}^{71}Ge$	0.233	pp, Be, B	$69.7 \pm 6.7^{+3.9}_{-4.5}$	131.5^{+21}_{-17}	122.5
Sage	$e - {}^{71}Ga \rightarrow \nu_e {}^{71}Ge$	0.233	pp, Be, B	72^{+12+5}_{-10-7}	131.5^{+21}_{-17}	122.5

Table 1: *Solar neutrinos: Data vs Standard Solar Model expectations. B-P: Bahcall and Pinsonneault[13] T-C-L: Turck-Chièze and Lopes[14]. Data are from Homestake[15], Gallex[16] Sage[17], and Kamiokande[18]. 1 SNU is defined to be one neutrino reaction per second in* 10^{36} *target atoms.*

the solar ν-flux observed by the ${}^{37}Cl$ experiment seemed[19] to show an anticorrelation with

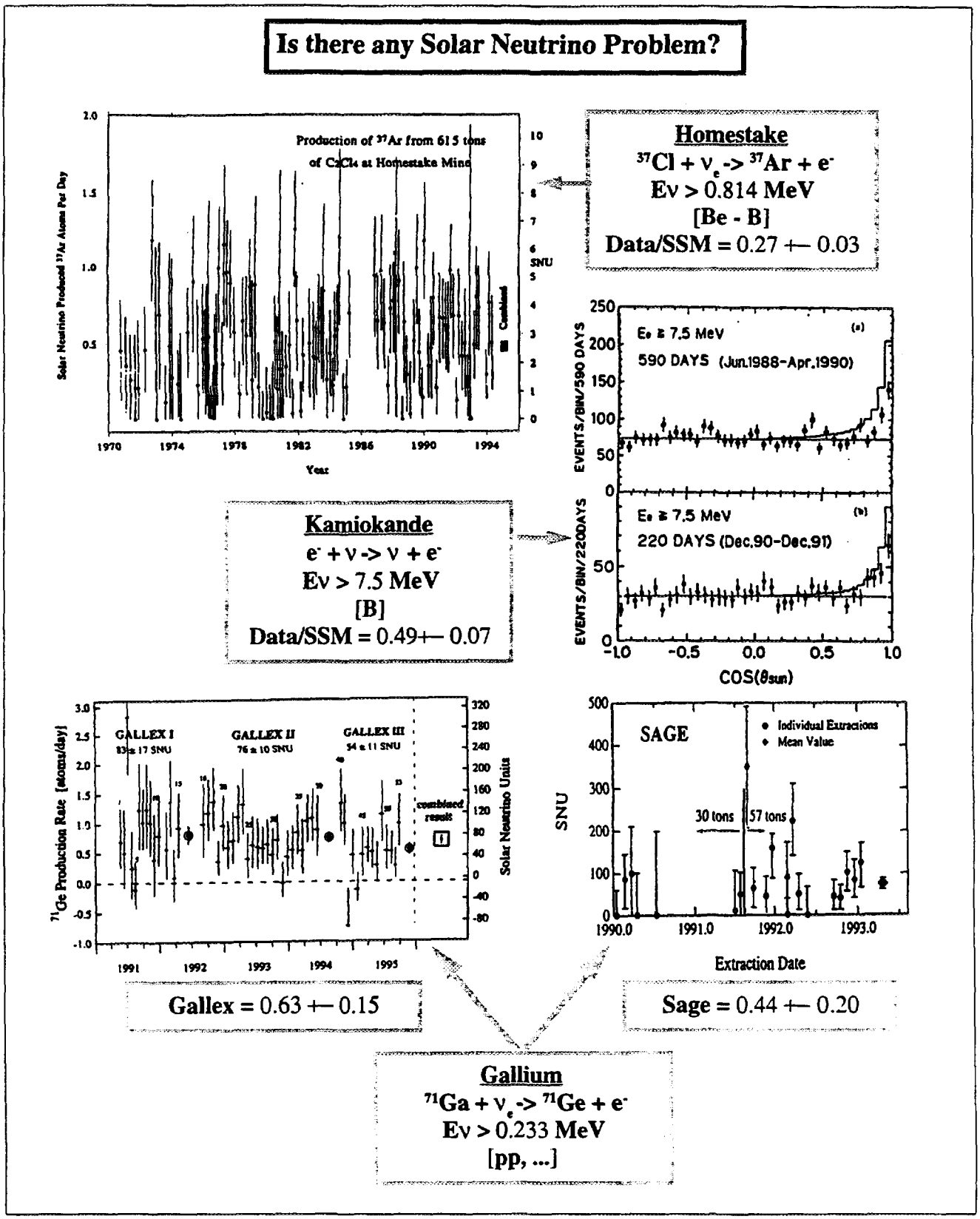

Figure 2: *Solar neutrino fluxes detected by various experiments and the Solar Neutrino Problem.*

the number of sunspots (Fig.3), which follows the 11 year period of the solar magnetic activity cycle. The convective zone of the sun contains currents responsible for toroidal magnetic fields, $B_\odot$. If the neutrino has a magnetic dipole moment, it undergoes spin precession in $B_\odot$ (see next chapter). Lefthanded neutrinos, which take part in the weak interaction, flip into righthanded, sterile, neutrinos. At high solar activity, i.e. maximum number of sunspots, the probability for spin flip is large, and hence less neutrinos would be detected on earth. At low solar activity, less neutrinos become sterile, and one would detect more neutrinos. The Kamiokande II water Cherenkov experiment does not see any anticorrelation (Fig.3), and in fact, even for Homestake the effect might be only a statistical fluctuation (at most 10% probability). The authors of Ref.[21] pointed out that the ^8B neutrinos should be modulated with a half-year period by the combined effect of the 7° inclination of the plane of the ecliptic to the solar equator and the weakening of the toroidal magnetic field near the equator. The toroidal field has opposite signs on different sides of the equator. The transition gap in the magnetic field, $\sim 7 \times 10^9\ cm$ shades the ^8B and ^8Be neutrinos produced in a small region near the center ($\sim 0.05 R_\odot \sim 3 \times 10^9\ cm$). The pp neutrinos are produced in a much more extended region $\sim 0.10 R_\odot$ up to $\sim 1.7 \times 10^{10}\ cm$. Results from Kamiokande and Gallex are discussed by W. Hampel[22]. Superkamiokande is a good candidate to follow these studies and look for such effects.

More recently, other indicators for the solar magnetic activity have been considered. McNutt[26] showed that there is an anticorrelation between the solar neutrino rates and the solar wind flux as measured near Earth by the MIT plasma experiment on the IMP 8 satellite. The surface magnetic flux[25, 27] has an advantage over sunspots in that it spans the whole solar disk. Oakley et al.[25] found, for the 2 solar cycles between 1970 and 1991, a "highly significant" anticorrelation between the Homestake data and the magnetograph-measured surface magnetic flux from the latitude zones centered on the solar disk, in the vicinity of the neutrino flight path. Fig.3 from reference[27],shows data from all 4 neutrino experiments plotted against the delayed magnetic flux. Interior fields travel to the solar surface in $\sim 0.3 - 1.4$ years. The question whether these anticorrelations might be only statistical fluctuations, requires data that span several solar cycles to answer.

If one beleives the experimental measurements, the question to ask is: is the Solar Neutrino Problem caused by unknown properties of neutrinos or by a lack of underdstanding of the interior of the sun? Is the deficit due to new physics or to faulty astrophysics? Here we assume the solar models[20] correct[2] and concentrate on the possibility for new physics. Solutions to the solar neutrino problem through neutrino oscillations (in vacuum or in matter) are addressed by S. Petcov[24] and W. Hampel[22]. Here we further consider neutrinos having electromagnetic properties.

2 Magnetic Moment and Spin Precession

2.1 Spin precession in vacuum

The evolution equation of a system with lefthanded ν_L and righthanded ν_R Dirac neutrinos in a magnetic field B is described by the Schrödinger-like equation

$$
\begin{aligned}
i\frac{d}{dx}\begin{pmatrix}\nu_L\\ \nu_R\end{pmatrix} &= \left[\begin{pmatrix}E_L & \mu B\\ \mu B & E_R\end{pmatrix}\right]\begin{pmatrix}\nu_L\\ \nu_R\end{pmatrix}\\
&= \left[p\begin{pmatrix}1 & 0\\ 0 & 1\end{pmatrix}+\begin{pmatrix}\frac{m_L^2}{2p} & \mu B\\ \mu B & \frac{m_R^2}{2p}\end{pmatrix}\right]\begin{pmatrix}\nu_L\\ \nu_R\end{pmatrix}\\
&= \left[\begin{pmatrix}\frac{\Delta_{LR}}{4E} & \mu B\\ \mu B & -\frac{\Delta_{LR}}{4E}\end{pmatrix}+\left(p+\frac{m_L^2+m_R^2}{4p}\right)\begin{pmatrix}1 & 0\\ 0 & 1\end{pmatrix}\right]\begin{pmatrix}\nu_L\\ \nu_R\end{pmatrix}
\end{aligned}
$$

where μ is the magnetic moment of the neutrino, $E = p\sqrt{1+\frac{m^2}{p^2}} \sim p\left(1+\frac{m^2}{2p^2}\right)$ its energy and $\Delta_{LR} = m_L^2 - m_R^2$. If we omit the terms proportional to the unit matrix, which are not responsible

[2] Dar and Shaviv claim that their model (see A. Dar in[23]) does reproduce the solar neutrino data. For Homestake, for example, they expect 0.2 *SNU* (*pep*), 0.9 *SNU* (^7Be), 2.7 *SNU* (^8B) and 0.3 *SNU* (*CNO*) (in total 4.1 *SNU*), whereas Bahcall and Pinsonneault[13] find 0.2, 1.2, 6.2 and 0.4 SNU, respectively (in total 8.0 *SNU*). The SNP problem is thus reduced to a "^8B neutrino problem". The situation is more complicated if gallium data are taken into account. One talks about a "^7Be neutrino problem", which cannot (yet?) be solved by non-standard solar models (see Ref.[22]).

for the spin precession, we obtain:

$$i\frac{d}{dx}\begin{pmatrix}\nu_L\\ \nu_R\end{pmatrix} = \left[\frac{\Delta_{LR}}{4E}\begin{pmatrix}1 & 0\\ 0 & -1\end{pmatrix}+\mu B\begin{pmatrix}0 & 1\\ 1 & 0\end{pmatrix}\right]\begin{pmatrix}\nu_L\\ \nu_R\end{pmatrix}$$
$$= \left(\frac{\Delta_{LR}}{4E}\sigma_3+\mu B\sigma_1\right)\begin{pmatrix}\nu_L\\ \nu_R\end{pmatrix}$$

The solution of the differential equation in the case of a uniform magnetic field B is

$$\begin{pmatrix}\nu_L(x)\\ \nu_R(x)\end{pmatrix} = \exp\left[-i\left(\frac{\Delta_{LR}}{4E}\sigma_3+\mu B\sigma_1\right)x\right]\cdot\begin{pmatrix}\nu_L(0)\\ \nu_R(0)\end{pmatrix}$$
$$= \left[\cos\Omega x-\frac{i}{\Omega}\left(\frac{\Delta_{LR}}{4E}\sigma_3+\mu B\sigma_1\right)\sin\Omega x\right]\cdot\begin{pmatrix}\nu_L(0)\\ \nu_R(0)\end{pmatrix}$$

where $\Omega^2 \equiv (\mu B)^2 + (\frac{\Delta_{LR}}{4E_\nu})^2$.

If at $x = 0$ there were only lefthanded Neutrinos ($\nu_R(0) = 0$), than after a distance x the probabilities to find a lefthanded neutrino or a righthanded neutrino are:

$$P_{\nu_L\nu_L}(x) = |<\nu_L(x)|\nu_L(0)>|^2 = |\cos\Omega x-\frac{i}{\Omega}\frac{\Delta_{LR}}{4E_\nu}\sin\Omega x|^2 = cos^2\Omega x + cos^2\beta\ sin^2\Omega x$$

$$P_{\nu_L\nu_R}(x) = |<\nu_R(x)|\nu_L(0)>|^2 = 1-P_{\nu_L\nu_L}(x) = sin^2\beta\ sin^2\Omega x$$

where $\tan\beta \equiv \frac{\mu B}{\Delta_{LR}/4E_\nu}$.

Efficient spin precession can be obtained[21] for $\beta \simeq 1$, giving $\Delta_{LR} \simeq 4E_\nu\ \mu\ B$. In the sun, where neutrinos are produced with an energy $E_\nu \sim 10\ MeV$ and assuming a magnetic field of $B \sim 10^3 - 10^4\ Gauss$, this leads to $|\ \Delta_{LR}\ | \simeq 10^{-7}\ eV^2$, for $\mu_\nu < 10^{-10}\mu_B$. This condition can be relaxed when matter effects are taken into account. From $\Omega x \sim \mu B x \sim 1$ and for $x \sim 2\times 10^{10}\ cm$ (solar convective zone) and $B \sim 10^3 - 10^4\ Gauss$, one would need $\mu \sim (0.1-1.0)\times 10^{-10}\mu_B$, in order to explain the solar neutrino deficit.

2.2 Spin precession in matter

In matter the neutrino gets an effective energy à la MSW[28, 29], due to its interaction with e^-, p and n (Fig.4)

$$H_\nu = H_{vac} + H_{int}$$

$$H_{int} = \sqrt{2}G_F\sum_f (I_3^f - 2Q_f\sin^2\theta_W)$$

	$I_3 - 2Q\sin^2\theta_W$	Effective energy $[V_\nu]$
Neutral Currents		
$\nu(e,p)\to\nu(e,p)$	cancel	0
$\nu n\to\nu n$	$-\frac{1}{2}$	$-\frac{G_F}{\sqrt{2}}n_n$
Charged Currents		
$\nu_e e^-\to\nu_e e^-$	$\frac{1}{2}+2\sin^2\theta_W$	$\sqrt{2}G_F n_e$

$$V_{\nu_e} = \sqrt{2}G_F(n_e-\frac{1}{2}n_n)\ ;\ V_{\nu_\mu} = -\frac{G_F}{\sqrt{2}}n_n$$

Only the lefthanded neutrino acquires an effective mass, the righthanded neutrino being sterile

$$\tilde{m}_L^2 = m_L^2 + 2\sqrt{2}G_F E_\nu\left(n_e-\tfrac{1}{2}n_n\right)\ ;\ \tilde{m}_R^2 = m_R^2$$

The condition for an efficient spin precession reads now

$$2\sqrt{2}G_F E_\nu\left(n_e-\frac{1}{2}n_n\right) \simeq 4E\mu B$$

$$\left(\left(n_e-\tfrac{1}{2}n_n\right)\le 10^{22}cm^{-3}\right) \Longrightarrow Solar\ Convective\ Zone!$$

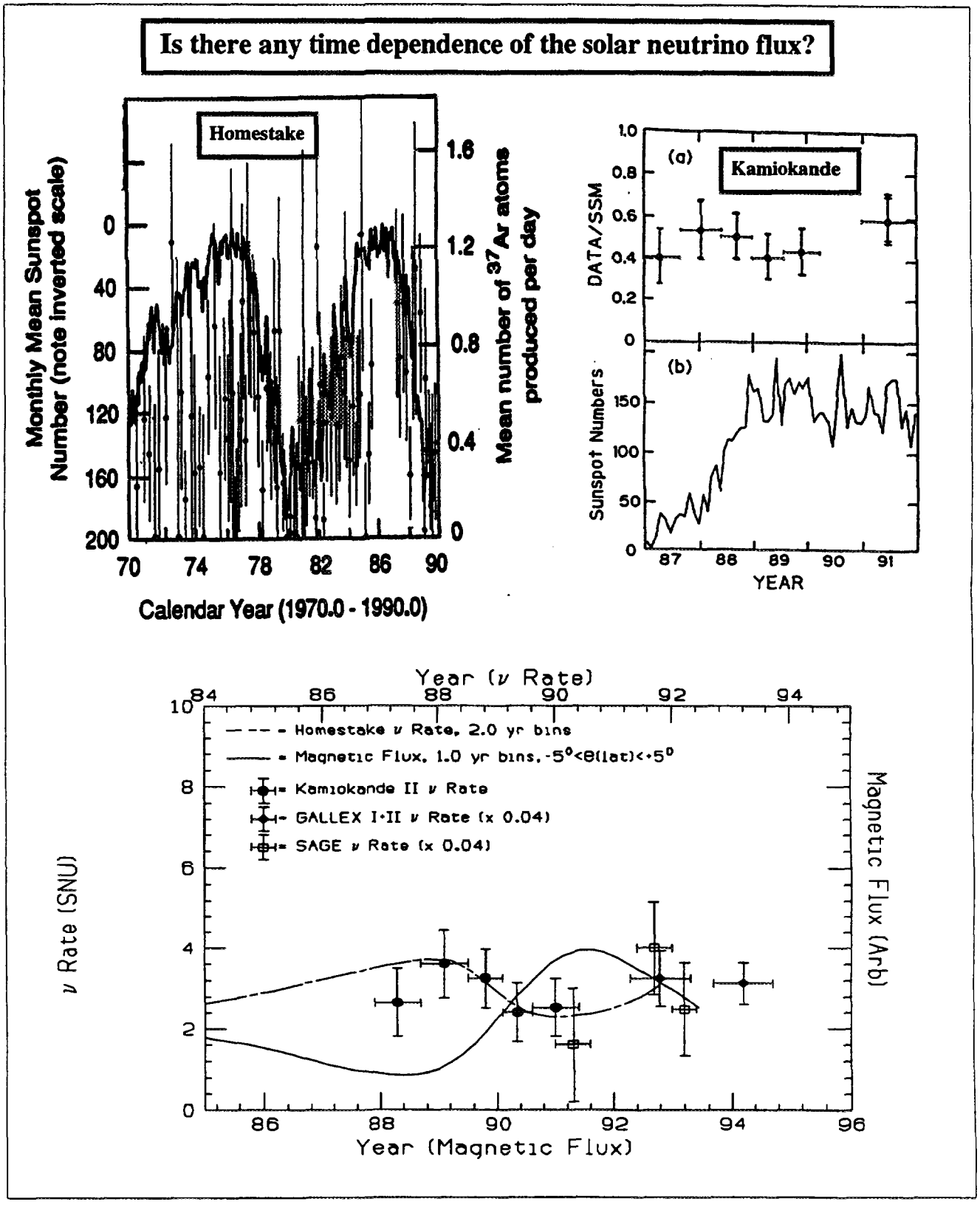

Figure 3: *Time evolution of the solar neutrino flux detected by various experiments compared to the number of sun spots (top) and to the solar magnetic flux. The magnetic scale is shifted by 1 year in order to plot a 1984 neutrino with a 1984 interior fiels, proxied by a 1985 surface field.*

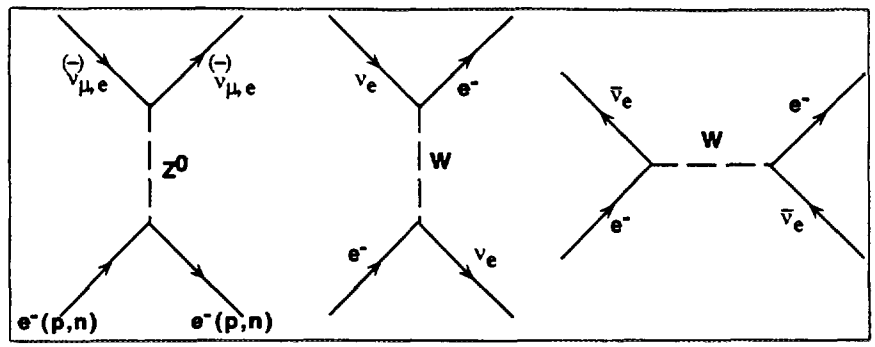

Figure 4: *Neutrino scattering off* e^-, p, n.

2.3 Resonant Spin-Flavour Precession

The effect [31, 33, 34] can be easily seen if two neutrino flavours are taken[41, 42].

The evolution equation in the case of 2 Dirac neutrinos and their antiparticles is

$$i\frac{d}{dx}\begin{pmatrix}\nu_{eL}\\ \nu_{\mu L}\\ \nu_{eR}\\ \nu_{\mu R}\end{pmatrix} = H\begin{pmatrix}\nu_{eL}\\ \nu_{\mu L}\\ \nu_{eR}\\ \nu_{\mu R}\end{pmatrix}$$

with

$$H = \begin{bmatrix} -\frac{\Delta m^2}{4E_\nu}\cos 2\theta + V_{\nu_e} & \frac{\Delta m^2}{4E_\nu}\sin 2\theta & \mu_{ee}B & \mu_{e\mu}B \\ \frac{\Delta m^2}{4E_\nu}\sin 2\theta & \frac{\Delta m^2}{4E_\nu}\cos 2\theta + V_{\nu_\mu} & \mu_{e\mu}B & \mu_{\mu\mu}B \\ \mu^*_{ee}B & \mu^*_{\mu e}B & -\frac{\Delta m^2}{4E_\nu} & 0 \\ \mu^*_{e\mu}B & \mu^*_{\mu\mu}B & 0 & +\frac{\Delta m^2}{4E_\nu} \end{bmatrix}$$

where

$$\Delta m^2 = m^2_{\nu_\mu} - m^2_{\nu_e}$$

In this case both diagonal (μ_{ll}) and transition moments ($\mu_{ll'}$) are possible. The right-handed neutrino is sterile, and hence no $\nu_{eR} - \nu_{\mu R}$ oscillations accur (no mixing). The crossing of diagonal elements are the regions where resonances occur:

- The SFP $\nu_{eL} - \nu_{\mu R}$ Resonance ($H_{11} = H_{44}$):

$$V_{\nu_e} = \frac{\Delta m^2}{4E}(1+\cos 2\theta) \Longrightarrow \left(n_e - \frac{1}{2}n_n\right)_R = \frac{\Delta m^2 \cos^2\theta}{2\sqrt{2}G_F E_\nu}$$

- The MSW $\nu_{eL} - \nu_{\mu L}$ Resonance ($H_{11} = H_{22}$):

$$(n_e)_R = \frac{\Delta m^2 \cos 2\theta}{2\sqrt{2}G_F E_\nu}$$

The condition for efficient precession with flavour mixing becomes: $\mid \Delta m^2 \mid \simeq 10^{-4}\ eV^2$.

The evolution equation in the case of 2 Majorana neutrinos and their antiparticles is

$$i\frac{d}{dx}\begin{pmatrix}\nu_{eL}\\ \nu_{\mu L}\\ \overline{\nu}_{eR}\\ \overline{\nu}_{\mu R}\end{pmatrix} = H\begin{pmatrix}\nu_{eL}\\ \nu_{\mu L}\\ \overline{\nu}_{eR}\\ \overline{\nu}_{\mu R}\end{pmatrix}$$

$$H = \begin{bmatrix} -\frac{\Delta m^2}{4E}\cos 2\theta + V_{\nu_e} & \frac{\Delta m^2}{4E_\nu}\sin 2\theta & 0 & \mu_{e\mu}B \\ \frac{\Delta m^2}{4E_\nu}\sin 2\theta & \frac{\Delta m^2}{4E_\nu}\cos 2\theta + V_{\nu_\mu} & -\mu_{e\mu}B & 0 \\ 0 & -\mu^*_{\mu e}B & -\frac{\Delta m^2}{4E_\nu}\cos 2\theta - V_{\nu_e} & \frac{\Delta m^2}{4E_\nu}\sin 2\theta \\ \mu^*_{e\mu}B & 0 & \frac{\Delta m^2}{4E_\nu}\sin 2\theta & \frac{\Delta m^2}{4E_\nu}\cos 2\theta - V_{\nu_\mu} \end{bmatrix}$$

In this case only transition moments ($\mu_{ll'}$) are possible; diagonal moments (μ_{ll}) must vanish. The right-handed neutrino ($\overline{\nu}_R = \nu_R$) interacts, and hence $\nu_{eR} - \nu_{\mu R}$ oscillations can accur.

It has been shown[35] that the three solar neutrino experiments could be reconciled for certain field configurations in the sun. A numerical integration of the evolution equation of the system $(\nu_e, \overline{\nu}_\mu)$ leads to the solution [$\Delta m^2 \sim 10^{-8}\ eV^2$; $\mu_\nu \sim 10^{-11}\ \mu_B$; $B_0 \sim 40kG$]. A better experimental measurement of μ_ν could therefore give more information about the magnetic field in the sun. Pulido[36] and Lim-Nunokawa[39] found a common solution to all solar neutrino experiments for a simple field configuration in the sun by taking into account the energy dependence of the survival probability $P_{\nu_e\nu_e}(x)$. Akhmedov[38] and Nunokawa-Minakata[37] treated the combined effect of the resonant spin-flavour precession and neutrino oscillations in matter.

The interest in measuring the dipole moment of the neutrino was triggered by the solar neutrino problem, especially the possible anticorrelation with the solar magnetic activity. Whether these are true is certainly questionable. It is nevertheless important to study a possible electromagnetic interaction of the neutrino, as part of its intrinsic properties. A non zero (Dirac) neutrino magnetic moment was postulated by Pauli[40] in the same letter in which the neutrino hypothesis was formulated.

Among the processes sensitive to the electromagnetic properties of the neutrino, we discuss νe^- scattering which presents two advantages: it is a pure weak, theoretically well understood process, and the recoil electron can be easily measured.

3 νe^- scattering

3.1 νe^- elastic scattering

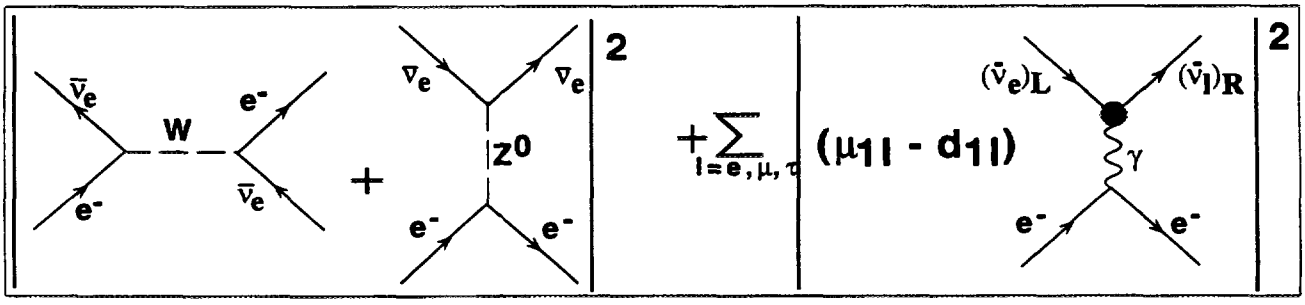

Figure 5: *Feynman diagrams contributing to $\overline{\nu}e^-$-Scattering.*

The differential cross-section for the elastic process $\nu e^- \to \nu e^-$ (Fig.5) gets two contributions: one from the weak interaction and one from a possible electromagnetic interaction of the neutrino[43, 44, 45]:

$$\frac{d\sigma}{dT} = \frac{d\sigma^W}{dT} + \frac{d\sigma^M}{dT}$$

$$\frac{d\sigma^W}{dT} = \frac{2G_F^2 m_e}{\pi}\left[g_L^2 + g_R^2(1 - \frac{T}{E_\nu})^2 - g_L g_R \frac{m_e T}{E_\nu^2}\right] \ ; \ \frac{d\sigma^M}{dT} = \frac{\pi\alpha^2}{m_e^2}\left(\frac{\mu_\nu}{\mu_B}\right)^2 \frac{1 - T/E_\nu}{T} \ ,$$

where $g_L = \frac{1}{2}[g'_V + g_A] = \frac{1}{2}[(g_V + x) + g_A]$ and $g_R = \frac{1}{2}[g'_V - g_A] = \frac{1}{2}[(g_V + x) - g_A]$.

$$g_V = \left\{ \begin{array}{c} 2\sin^2\theta_W + 1/2 \\ 2\sin^2\theta_W - 1/2 \end{array} \right\} \ , \ g_A = \left\{ \begin{array}{c} +1/2 \\ -1/2 \end{array} \right\} \ for \left(\begin{array}{c} \nu_e e^- \\ \nu_\mu e^- \ ; \ \nu_\tau e^- \end{array} \right)$$

$$\left\{ \begin{array}{l} g_L \leftrightarrow g_R \\ g_A \rightarrow -g_A \end{array} \right\} \; for \; \overline{\nu} e^-$$

The other parameters are T : kinetic energy of the recoil electron, E_ν : energy of the incoming neutrino, G_F : Fermi constant, α : QED coupling constant, and θ_W : Weinberg weak mixing angle ($\sin^2\theta_W \sim 0.23$). An intrinsic neutrino charge radius, indicating an internal structure of the neutrino would manifest itself as a shift, x, of the weak neutral current vector coupling, g_V

$$x = \frac{\sqrt{2}\pi\alpha}{3G_F}\langle r^2\rangle = \frac{2M_W^2}{3}\sin^2\theta_W\langle r^2\rangle \sim 2.38\times 10^{30} cm^{-2}\langle r^2\rangle.$$

Other shifts due to radiative corrections within the standard model are predicted to be small[49], of the order of -0.004. Note that high neutrino energies are better suited to set limits on this quantity.

The one-photon exchange mechanism leads to a spin-flip of the outgoing leptons, therefore the electromagnetic and weak contributions to the toal cross section do not interfere, and the neutrino magnetic moment leads to an increase of the event rate. Notice that the constant electromagnetic term, $\frac{\pi\alpha^2}{m_e^2} \sim 2.5\times 10^{-25}$, is much larger than the weak cross section. A measurement of μ_ν consists in looking for deviations from purely weak processes.

The weak νe and $\overline{\nu} e$ elastic cross sections increase linearly with the neutrino energy: $\sigma \sim (0.14 - 0.9)\times 10^{-44}[E_\nu/MeV]\ cm^2$. As a comparison the νN cross-sections are proportional to E^2: $\sigma(\overline{\nu}_e p \rightarrow e^+ n) \sim \sigma(\nu_e n \rightarrow e^- p) \simeq 9.75\times 10^{-44}[E_\nu/MeV]^2\ cm^2$ for $E_\nu \ll m_N$.

The electromagnetic cross section, on the other hand, rises only logarithmically with the neutrino energy E_ν $\sigma^M \sim \ln E_\nu$. Therefore, it is advantageous to perform experiments searching for a magnetic moment of the neutrino at low energies. Reactors, with an antineutrino energy spectrum peaking around 1 MeV, are more suitable than accelerators.

The quantities to be measured experimentally are the recoil kinetic energy T_e and the scattering angle θ_e of the electron. These are related by

$$\cos\theta_e = \frac{E_\nu + m_e}{E_\nu}\sqrt{\frac{T_e}{T_e + 2m_e}} \;\; ; \;\; T_e = m_e \frac{E_\nu^2\cos^2\theta_e}{E_\nu + m_e/2 + (E_\nu^2\sin^2\theta_e)/2m_e}$$

The maximal recoil (Compton edge) is for electrons emitted in the forward direction ($\theta_e = 0°$)

$$T_e^{max} = \frac{2E_\nu^2}{2E_\nu + m_e}$$

The differential cross-section for $\overline{\nu}_e e \rightarrow \overline{\nu}_e e$, averaged over the antineutrino spectrum[45], as function of the recoil electron energy T_e, is

$$\langle\frac{d\sigma}{dT_e}\rangle = \int_{E_\nu^{min}(T_e)}^{\infty} \frac{dN_\nu}{dE_\nu}\frac{d\sigma}{dT_e}dE_\nu$$

The ratio of the total and weak integrated cross sections are depicted in Fig.6 for different values of μ_ν. $\sin^2\theta_W = 0.226$ was used. One can see why it is important to go to lower energies to probe the magnetic moment of the neutrino. Furthermore, the electromagnetic cross section is more strongly peaked in the forward direction than the weak cross section The goal of a precision experiment is, therefore, to measure both the energy and the angular distribution of the recoil electron.

3.2 Dynamical zero in $\overline{\nu} e^-$ elastic scattering

The weak contribution to the differential cross-section for the elastic process $\overline{\nu}_e e^- \rightarrow \overline{\nu}_e e^-$ is given by

$$\frac{d\sigma^W}{dT_e} = \frac{2G_F^2 m_e}{\pi}\left[g_R^2 + g_L^2(1 - \frac{T_e}{E_\nu})^2 - g_L g_R \frac{m_e T_e}{E_\nu^2}\right]$$

For forward electrons with a maximal recoil T_e^{max} one obtains

$$\frac{d\sigma^W}{dT_e} = \frac{2G_F^2 m_e}{\pi}\left[g_R - g_l\frac{m_e}{2E_\nu + m_e}\right]^2$$

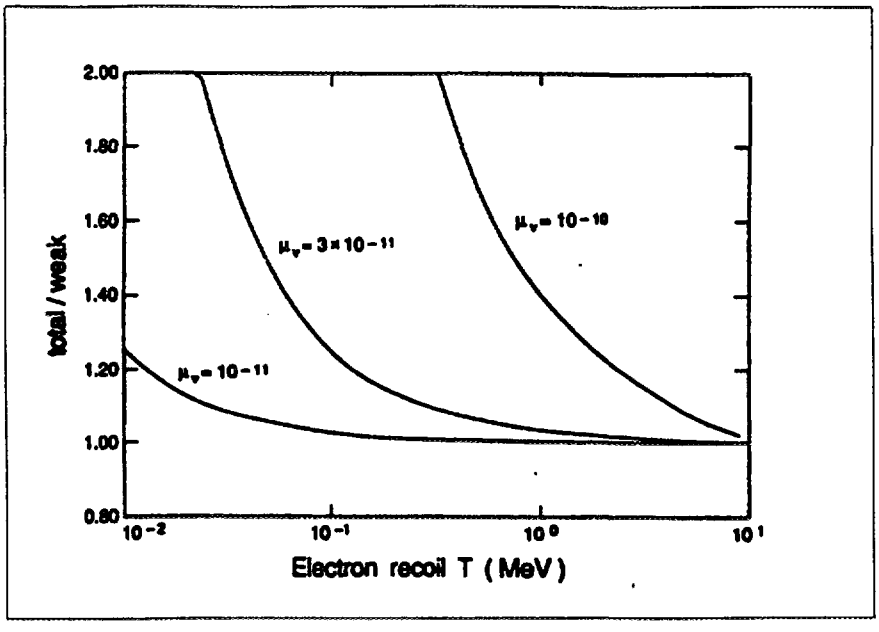

Figure 6: *Ratio of total to weak cross-sections for $\overline{\nu}_e e^- \to \overline{\nu}_e e^-$, averaged over the antineutrino spectrum, as a function of the electron recoil energy. Different value of μ_ν are considered*

which can vanish if the following condition is fulfilled

$$\left(\frac{d\sigma^W}{dT_e}\right)_{forward} = 0 \Longrightarrow g_R = g_l \frac{m_e}{2E_\nu + m_e} \Longrightarrow E_\nu = \frac{g_L - g_R}{2g_R} m_e$$

With $g_L = 2\sin^2\Theta_W + 1$ and $g_R = 2\sin^2\Theta_W$, the condition for dynamical zero reads $E_\nu = \frac{m_e}{4\sin^2\Theta_W} \sim 500\ keV$. It is interesting to see that these $\overline{\nu}$-energies are provided by reactors. The corresponding maximal recoil energies, $T_e^{max} \sim 350\ keV$, could be measured by the MUNU detector, as we will see later on. As the electromagnetic contribution to the cross-section is not affected by the dynamical zero, the study of forward electrons is sensitive to a hypothetical magnetic moment of the neutrino. Such an experiment requires high rates and good energy and angular resolutions. Notice that for all other types of neutrinos ($\nu_{e,\mu,\tau}, \overline{\nu}_{\mu,\tau}$) there is no cancellation. As a consequence oscillations $\overline{\nu}_e \leftrightarrow \overline{\nu}_\mu$ can be performed. The authors of Ref.[46, 47] showed results that could be obtained with a detector (of type MUNU) sitting 20 meters from the core of a reactor. The bounds could be comparable to that obtained for $\nu_e \leftrightarrow \nu_\mu$ oscillations by atmospheric neutrino detectors.

3.3 $\overline{\nu}e^-$ inelastic scattering

In the case of elastic scattering $\overline{\nu}_e e^- \to \overline{\nu}_e e^-$ the sensitivity to the magnetic moment is limited by the threshold T_e^{min} ($\sim 300 - 500\ keV$ for MUNU): $Q^2 = 2m_e T_e \geq 2m_e T_e^{min}$. In the inelastic case (Fig.7) $\overline{\nu}_e e^- \to \overline{\nu}_e e^- \gamma$, there is no Q^2 limitation. The normalised quantity

$$x = \frac{Q^2}{2m_e(T_e + T_\gamma)}$$

can take values between 0 and 1. This enhances the sensitivity to μ_ν. Experimentally, however, it is necessary to measure the photon energy, and the rates are suppressed by a factor α.

The authors of reference [48, 47]) computed the ratio of the magnetic and weak differential cross sections as function of x and $\nu = T_e + E_\gamma$ for $\mu_\nu = 10^{-10}\mu_B$, by taking into account the reactor spectrum. The threshold energies assumed are $T_e^{min} = 100\ keV$ and $E_\gamma^{min} = 100\ keV$. For $\nu \leq 0.5\ MeV$ and $x \leq 0.5$, the electromagnetic cross section is $\sigma_M = 2.7 \times 10^{-47} cm^2$, and is 4.4 times larger than the weak cross section σ_W.

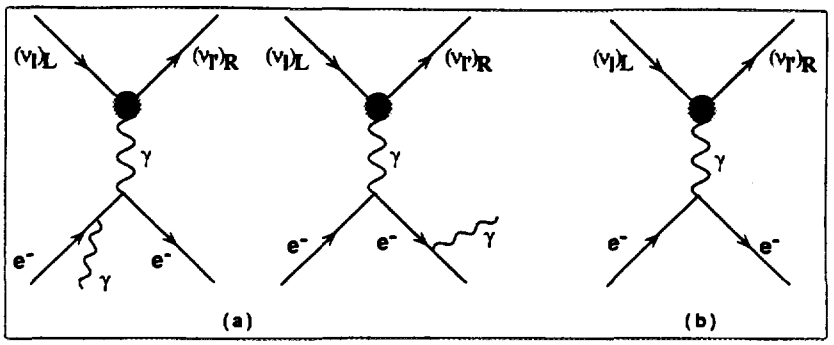

Figure 7: *Electromagnetic interaction Feynman diagrams contributing to νe^- inelastic (a) and elastic (b) scattering.*

4 Experimental Limits

4.1 Laboratory limits

4.1.1 Reactor experiments

The neutrino (in fact $\overline{\nu}_e$) was experimentally discovered in 1956 at the Savannah River nuclear reactor[2], by observing the reaction $\overline{\nu}p \rightarrow ne^+$ The reactor power was 1800 MW corresponding to a neutrino flux of $1.9 \times 10^{13} \frac{\overline{\nu}}{cm^2 \cdot s}$. The detector consisted of a large liquid scintillator, of high hydrogen content and loaded with a cadmium compound. Positrons lead to prompt scintillations while photons from the absorbtion of neutrons in cadmium give delayed pulses with predictable energy and time delay spectra.

Savannah River Reactor

The reaction $\overline{\nu}_e e^- \rightarrow \overline{\nu}_e e^-$ was first observed at the Savannah River nuclear plant[54]. The experiment used a segmented 15.9 kg plastic scintillator (CH_2), surrounded by an anti-Compton, NaI counter to suppress the γ background, a lead shield and a liquid scintillator to veto cosmics. A Signal event was defined by a single count in one of the elements of the plastic scintillator with nothing in coincidence. Annihilation γ rays and neutrons from reaction $\overline{\nu_e}p \rightarrow e^+n$ (200 events/day in the plastic scintillator) were detected or identified by the delayed neutron capture signal in the plastic scintillator or in NaI. Assuming a vanishing magnetic moment, the experiment lead to a measurement of the Weinberg weak angle $\sin^2\theta_W = 0.29 \pm 0.05$. With today's improved knowledge on both the Weinberg angle and the reactor spectrum Vogel and Engel[45] obtained a magnetic moment $\mu_{\nu_e} \sim 3 \times 10^{-10}\mu_B$, with a significance of about 3σ! The main limitation of the experiment was the short running time (2 months) and the high electron detection threshold (1 MeV).

	$\bar{\nu}_e$ events/day			
Reactor	T[MeV]	Reactor on	Reactor off	on-off
Savannah		(64.6 days)	(60.7 days)	
($P = 1800\ MW$				
$1.9 \times 10^{13}\overline{\nu}/cm^2 \cdot s$	$1.5 - 3.0$	45.1 ± 1.0	39.2 ± 0.9	5.9 ± 1.4
$11.2\ m$ from core)	$3.0 - 4.5$	2.4 ± 0.19	1.2 ± 0.14	1.2 ± 0.25
Kurchatov		(254 days)	(78 days)	
$P = 2000\ MW$				
$2.7 \times 10^{12}\overline{\nu}/cm^2 \cdot s$	$3.15 - 5.17$	8.27 ± 0.18	7.49 ± 0.31	0.78 ± 0.36
Rovno		(29.6 days)	(16.7 days)	
$(2 \times 10^{13}\overline{\nu}/cm^2 \cdot s$	$0.6 - 2.0$	4962 ± 12	4921 ± 16	41 ± 20
$15\ m$ from core)	$1.3 - 2.0$	508.5 ± 4.0	503.3 ± 5.6	5.2 ± 6.8

Table 2: *Event Rates in the Savannah River, Kurchatov and Rovno reactor experiments[54, 55, 56].*

Kurchatov Reactor

A more recent experiment at the Kurchatov Institute in Moscow[55] used seven cells filled with a C_6F_6 based liquid scintillator (103 kg) as active target material, containing 3×10^{28} electrons. The number of hydrogen atoms in the scintillator is 1.6×10^{25}. The detector is surrounded by various shielding layers, to suppress background from local activities, and by a plastic scintillator

on the top to veto cosmic rays. The reactor power and the neutrino flux are 2000 MW and $3.4 \times 10^{12} \frac{\bar{\nu}}{cm^2 \cdot s}$, respectively. The signal to noise ratio is $S/N \sim 1/10$ in the energy domain $3.15 \leq T_e \leq 5.175$ (it was $\sim 1/50$ at the beginning of the experiment.). The measured $\bar{\nu}e^-$ total cross section is: $\sigma_{\bar{\nu}e} = (4.5 \pm 2.4) \times 10^{-46} cm^2$/fission, giving, in the framework of the standard model, a value for the Weinberg-angle of: $\sin^2\theta_W = 0.22^{+0.7}_{-0.8}$. The upper limit for the magnetic moment obtained so far ($\sin^2\theta_W = 0.23$ as input) is

$$\mu_{\nu_e} < 2.4 \times 10^{-10} \mu_B \ , \quad CL = 90\%$$

limited by background and the low reactor flux. The experiment gives an upper limit on the neutrino charge radius of

$$|r_{\nu_e}| < 2.7 \times 10^{-16} cm \ , \quad CL = 90\%$$

Rovno Reactor

Derbin et al.[56] used a 75 kg silicon multidetector which consisted of 600 Si(Li) modules, 30 mm

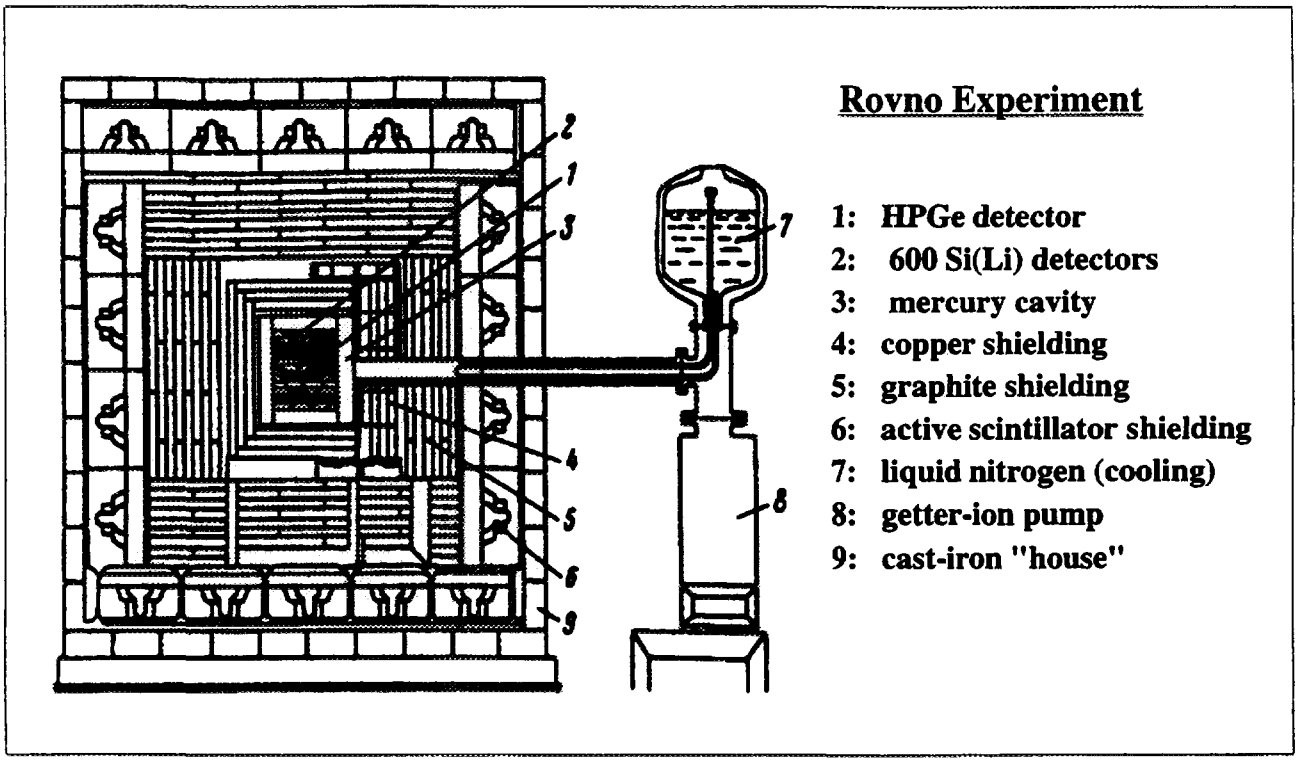

Figure 8: *Experimental setup at the Rovno nuclear power plant.*

in diameter and 125 mm long each. The multidetector (Fig.8) is surrounded by an active shielding (120 plastic scintillators $2.5 \times 2.5 \times 2.0\ m^3$) and by various passive shielding layers (80 mm mercury, 150 mm copper, 500 mm graphite, a cadmium absorber and 150 mm iron). The neutrino flux of the reactor (VVR-100) is $2 \times 10^{13} \frac{\bar{\nu}}{cm^2 \cdot s}$ and the detector is 15 m away from the core. The count rates obtained with 37.5 kg detector[3] during 29.6 days (reactor ON) and 16.7 days (reactor OFF) are summarised in Tab.3 for various energy intervals. Notice the very low signal to noise ratio. The cross section measured in the interval $0.6 - 2.0\ MeV$ is: $\sigma_{\bar{\nu}e} = (1.26 \pm 0.62) \times 10^{-44} cm^2$/fission, corresponding to $\sigma_{\bar{\nu}e} = (1.28 \pm 0.63) \times \sigma_{weak}$ ($\sin^2\theta_W = 0.22$ assumed). Allowing for a magnetic interaction, the following upper limit was obtained

$$\mu_{\nu_e} < 1.8 \times 10^{-10} \mu_B \ , \quad CL = 90\%$$

[3] By studying the distribution of the count rate as a function of the lower threshold, it was found that the dispersion exceeded that expected statistically up to 0.6 MeV. Half of the detectors were thus removed.

	events/day				
T[MeV]	Reactor on	Reactor off	on-off	$\mu_\nu = 0$	$\mu_\nu = 2 \times 10^{-10}$
0.2-2.0	15327 ± 92	14878 ± 90	449 ± 130	62	178
0.3-2.0	11193 ± 70	10908 ± 70	285 ± 98	53	128
0.6-2.0	4962 ± 12	4921 ± 16	41 ± 20	32	54
1.3-2.0	508.5 ± 4.0	503.3 ± 5.6	5.2 ± 6.8	8.9	10

Table 3: *Count rates measured by the Rovno experiment with 37.5 kg detectors [56].*

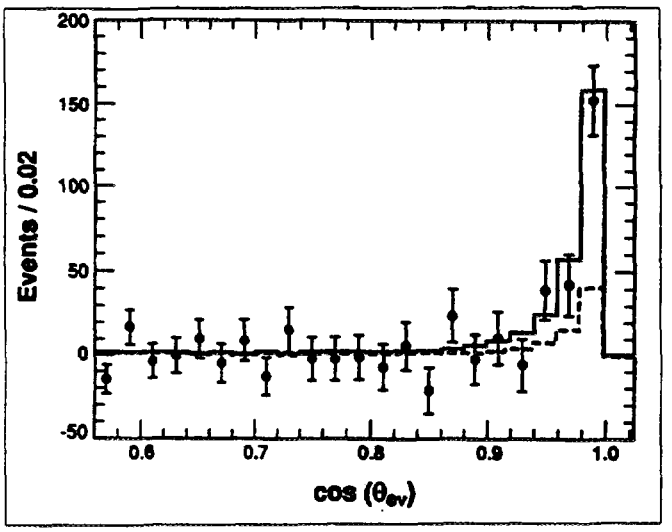

Figure 9: *Angular distribution of the νe elastic scattering signal measured by E225. The solid line is the result of the best fit,* 295 ± 35 *events. The dotted line is the background contribution from the* 59.2 $(\nu_\mu + \overline{\nu}_\mu)e^-$ *scattering events.*

4.1.2 Accelerator experiments

Beam dump experiments at accelerators produce intermediate and high energy neutrinos through the decay of pions: $\pi^+ \to \mu^+\nu_\mu$, $\mu^- \to e^-\overline{\nu}_e\nu_\mu$. The fact that the ν_e are accompanied by ν_μ and $\overline{\nu}_\mu$ complicates the interpretation of the data.

Los Alamos Meson Physics Facility (LAMPF)

Neutrinos are emitted isotropically by pion decay at rest ($\pi^+ \to \mu^+\nu_\mu$), followed by muon decay at rest ($\mu^+ \to e^+\overline{\nu}_\mu\nu_e$), in the 800 MeV proton beam stop. The muon neutrinos are produced with an energy of 29.8 MeV, whereas ν_e and $\overline{\nu}_\mu$ have a maximum energy of 52 MeV. For the beam exposure of 1.12×10^{23} protons, the time integrated neutrino flux for each of the 3 neutrino types was $(9.16 \pm 0.67) \times 10^{14}/cm^2$ at the average detector distance from the beam stop of ~ 9 m.

The E225 experiment aimed to measure the NC-CC interference, I, in $\nu_e e^-$-scattering. The central detector consisted of 40 plastic scintillation planes containing $(4.94 \pm 0.05) \times 10^{30}$ target electrons (energy loss measurement), interleaved by flash chamber modules to measure the position and direction of the particles. It is surrounded by massive shielding and high-efficiency cosmic-ray anticoincidence counters. The other sources of background are neutron capture and $\nu_e C$ reactions. 295 ± 35 $\nu_e e^-$ events are observed with a contribution of 59 events due to $(\nu_\mu + \overline{\nu}_\mu)e^-$ scattering (Fig.9). A neutrino flux-weighted cross section of $\sigma(\nu_e e^-) = (3.18 \pm 0.48 \pm 0.29) \times 10^{-43} cm^2$ is obtained. This is equivalent to $\sigma(\nu_e e^-)/E_\nu = (10.0 \pm 1.5 \pm 0.9) \times 10^{-45} cm^2/MeV$ at a mean neutrino energy $< E_\nu >= 31.7$ MeV. The interfernce term is obtained after subtracting the NC and CC contributions $I = -1.07 \pm 0.17 \pm 0.11$, in good agreement with the standard model prediction (assuming $\sin^2\theta_W = 0.233$) of $I = 4g_L = -2 + 4\sin^2\theta_W = -1.07$. A magnetic moment contribution has been tested for both ν_e and ν_μ. The angular distribution consisted of 274 ± 37 νe events, 626 $\nu^{12}C$ events, 136 other ν-nuclear interactions, and 442 ± 75 remaining neutron induced background events. An energy threshold of 10 MeV was used. Comparing the SM rate, $R_{SM} = 285$ asuming $\sin^2\theta_W = 0.227$, to the observed rate of 274 ± 37, there are fewer than 68 events ($CL = 90\%$) due to magnetic scattering. These are interpreted as the following limits on

μ_ν[57, 53]

$$\begin{aligned} \mu_{\nu_e} &< 1.08 \times 10^{-9}\mu_B\ , \quad CL = 90\% \qquad (\mu_{\nu_\mu} = 0) \\ \mu_{\nu_\mu} &< 7.4 \times 10^{-10}\mu_B\ , \quad CL = 90\% \qquad (\mu_{\nu_e} = 0) \\ \mu_\nu &< 6.1 \times 10^{-10}\mu_B\ , \quad CL = 90\% \quad (\mu_\nu = \mu_{\nu_e} = \mu_{\nu_\mu}) \end{aligned}$$

The experiment gives an upper limit on the neutrino charge radius of

$$-3.56 \times 10^{-32} cm^2 < |r_\nu|^2 < 5.44 \times 10^{-32} cm^2\ ;\ |r_\nu| < 2.3 \times 10^{-16} cm\ \ (CL = 90\%)$$

Alternating Gradient Synchrotron (AGS at BNL)

The wide band neutrino (antineutrino) beam is produced with a mean energy of 1.3 GeV by 28.3 GeV protons. The E734 experiment at Brookhaven National Laboratory accumulated $159 \pm 17.3 \pm 3.7$ $\nu_\mu e^-$ and $96.7 \pm 13.2 \pm 4.7$ $\overline{\nu}_\mu e^-$ events between 1981 and 1986. The 170 ton-detector consisted of a target calorimeter (112 planes of liquid scintillator and 2 planes of proportional drift tubes) followed by a gamma catcher and a muon spectrometer. The following results have been obtained[52]

$$\mu_{\nu_\mu} < 8.5 \times 10^{-10}\mu_B\ \ (CL = 90\%)\ ;\ -2.11 \times 10^{-32} cm^2 < |r_\nu|^2 < 0.24 \times 10^{-32} cm^2$$

or $\sin^2\theta_W = 0.195 \pm 0.018 \pm 0.013$.

Super Proton Sychrotron (SPS at CERN)

The CHARM II experiment at the CERN-SPS wide band beam (450 GeV protons) produced neutrinos with energies ranging from 0 to 120 GeV ($< E_\nu > \sim 25\ GeV$). The detector consisted of a 600 ton target calorimeter (420 glass plates, 5 cm thick, interspaced by planes of limited streamer tubes), preceded by a veto system with iron plates and scintillator hodoscope, and followed by a muon spectrometer. Between 1987 and 1991, more than 5000 $(\nu_\mu + \overline{\nu}_\mu)e^-$ events were accumulated. The quantities μ_ν and $< r_\nu^2 >$ were obtained from a fit of modelled differential distributions in E_e and $E_e\theta_e^2$ to the data ($E_e > 3\ GeV$). The fit yields[58] $\mu_{\nu_\mu} = \left[1.5^{+0.4}_{-0.6}(stat.)^{+0.8}_{-1.3}(syst.)\right] \times 10^{-9}\mu_B$. Adding statistical and systematical errors in quadrature, the result is compatible with zero with the upper limit

$$\mu_{\nu_\mu} < 3 \times 10^{-9}\mu_B\ ,\ \ CL = 90\%$$

The electroweak mixing angle was found to be $\sin^2\theta_W = 0.2324 \pm 0.0062 \pm 0.0059$. A comparison to the value measured at LEP, $\sin^2\theta_W^{eff} = 0.2324 \pm 0.0005$, leads to a value of the anomalous charge radius of the muon neutrino of $|r_\nu|^2 = (0.4 \pm 3.7) \times 10^{-33} cm^2$, corresponding to the upper bounds

$$|r_\nu|^2 < 0.6 \times 10^{-32} cm^2\ \ ;\ \ |r_\nu| < 0.77 \times 10^{-16} cm\ \ (CL = 90\%)$$

The best upper limits on the magnetic moment of the tau-neutrino are obtained by Cooper et al.[60] in a reanalysis of the data taken in 1982 by the WA66 experiment at Cern/SPS, using the Big European Bubble Chamber (BEBC)[61], to look for $\nu_\tau e^- \to \nu_\tau e^-$. A beam of 400 GeV protons from SPS was dumped onto a high density target (copper block, 404 m upstream of BEBC) which absorbed most of the long-lived secondaries (π, K) thus suppressing the conventional flux of decay neutrinos. The neutrino beam was hence enriched in neutrinos from decays of short-lived hadrons, $D^\pm$, D^0, $\overline{D}^0$, Λ_c, and D_s: $D_s \to \tau\nu_\tau$; $\tau \to \nu_\tau X$. Three events were found (visible momentum above 0.5 GeV), 2 with an e^+ and 1 with an e^-, with no observed hadrons in the final state. The 2 e^+ events are consistent with background from $\overline{\nu_e}p \to e^+n$. The e^- has a momentum of 3.7 GeV/c and is emitted in the forward direction (20 ± 15 $mrad$), consistent with $\nu e^- \to \nu e^-$. With one event observed and 0.5 ± 0.1 predicted by the standard model with $\sin^2\theta_W = 0.23$, a 90% CL upper limit of 3.5 events could be attributed to any other production processes. Recent measurements of charm production and charmed meson decay branching ratios were taken into account in order to estimate the ν_τ-flux: The following ingredients were used as inputs: $\sigma(pp \to D\overline{D} + X) = 13\ \mu b$,

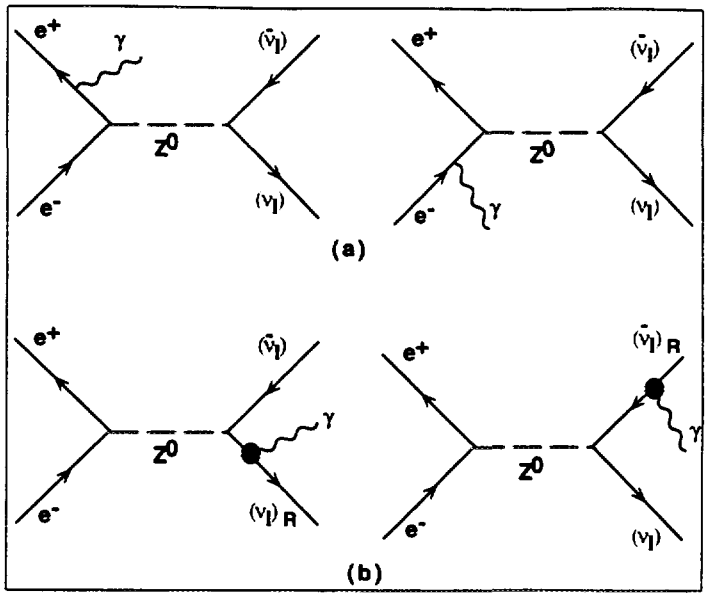

Figure 10: *Feynman diagrams contributing to $e^+e^- \to \nu\bar{\nu}\gamma$: (a) in the standard model (initial state photon radiation); (b) with a contribution from a magnetic interaction of the neutrino (final state radiation).*

$\sigma(pp \to \Lambda_c\overline{D} + X) = 5\ \mu b$, $\sigma(D_s\overline{D}_s)/\sigma(D\overline{D}) = 0.1$, $BR(D_s \to \tau\nu_\tau) = 4.83^{+0.38}_{-0.31}\%$ (obtained by scaling from $\pi \to \mu\nu_\mu$ using the D_s lifetime $\tau_{D_s} = 4.45^{+0.35}_{-0.29} \times 10^{-13}s$). Assuming $\mu_\nu = 10^{-6}\mu_B$, $14.8^{+1.5}_{-1.2}$ events were expected ($E_\nu > 1\ GeV$).The 90% CL upper limit translates to

$$\mu_{\nu_\tau} < 5.4 \times 10^{-7}\mu_B\ ,\quad CL = 90\%$$

which, however, requires assumptions on the D_s production cross section and its branching ratio into $\tau\nu_\tau$, which are not yet measured.

e^+e^--colliders (PEP, PETRA, LEP)

The process $e^+e^- \to \nu\bar{\nu}\gamma$, in which the only final-state particle detected is a photon, proceeds through the exchange of a Z^0 boson. In the standard model the single photon is emitted by the $e^\pm$ (Fig.10(a)). Near the Z resonance, the energy carried by a photon from initial-state radiation tends to be a few GeV at most. A magnetic interaction of the neutrino would manifest itself through a photon emission by the final-state $\nu\bar{\nu}$ (Fig.10(b)). These photons would carry a sizable fraction of the beam energy.

The best limit comes from single photon searches at PEP and PETRA. Data from ASP, MAC, CELLO and MARKJ experiments have been used to obtain the bounds [62]

$$\mu_{\nu_\tau} < 4 \times 10^{-6}\mu_B\ ,\quad CL = 90\%$$

A similar work using data taken in 1990 an 1991 by the ALEPH and L3 experiments [63] resulted in $\mu_{\nu_\tau} < 5.5 \times 10^{-6}\mu_B\ , CL = 90\%$.

The L3 collaboration reported recently on a search for energetic single-photon events ($E_\gamma > 15\ GeV$) in the data collected at LEP in 1991-1993. Fig.11 shows the energy distribution of the single photons. The data are compared to the standard model only (solid histogram) and to the SM with a possible magnetic contribution $\nu_\tau = 5 \times 10^{-6}\mu_B$ (dashed histogram). Requiring the photon energy to be greater than one half the beam energy, L3 obtains the limit[64] $\mu_{\nu_\tau} < 4.1 \times 10^{-6}\mu_B$ ($CL = 90\%$).

The experimental upper limits in reactor and accelerator experiments are summarised in Tab.5, together with the astrophysical bounds, we will discuss in the next chapter. To be complete, upper limits on the charge radius squared of the neutrino are given in Tab.4.

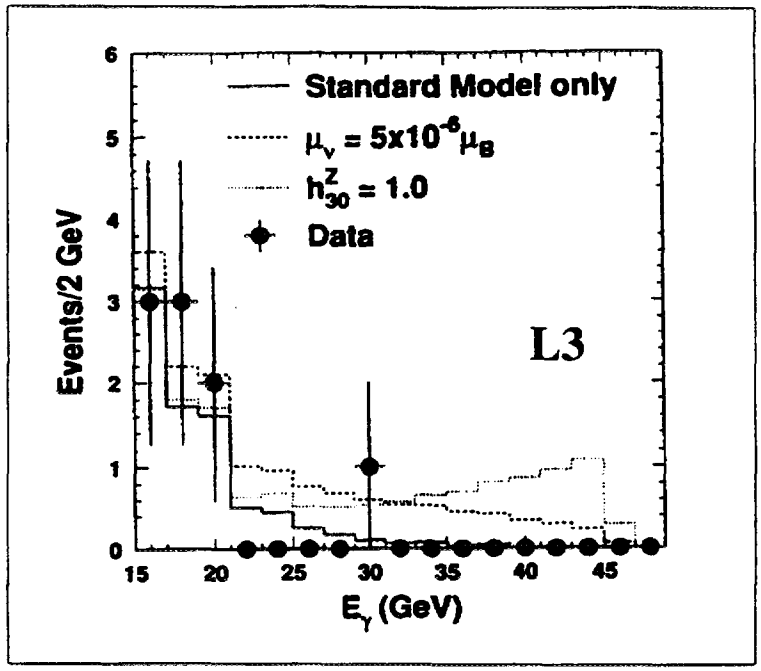

Figure 11: *Energy spectrum of single photon event search from L3 at LEP[64]. The data are compared to the standard model only (solid histogram), SM with a contribution from* $\nu_\tau = 5 \times 10^{-6}\mu_B$ *(dashed histogram), SM extention including an anomalous* $ZZ\gamma$ *coupling (dotted histogram))*

$\nu_\mu e^- \to \nu_\mu e^-$ [50]	$\langle r^2_{\nu_\mu}\rangle < 0.81 \times 10^{-32} cm^2 \quad (\langle r^2_{\nu_\mu}\rangle > 0)$
	$\langle r^2_{\nu_\mu}\rangle > -7.3 \times 10^{-32} cm^2 \quad (\langle r^2_{\nu_\mu}\rangle < 0)$
$\nu_\mu e^- \to \nu_\mu e^-$ [51]	$\langle r^2_{\nu_\mu}\rangle = (-0.3 \pm 1.5) \times 10^{-32} cm^2$
$\nu_\mu e^- \to \nu_\mu e^-$ [52]	$\langle r^2_{\nu_\mu}\rangle = (-1.1 \pm 1.0) \times 10^{-32} cm^2$
$\nu_e e^- \to \nu_e e^-$ [53]	$\langle r^2_{\nu_e}\rangle = (0.9 \pm 2.7) \times 10^{-32} cm^2$
$\overline{\nu}_e e^- \to \overline{\nu}_e e^-$ (Reactor)[55]	$\langle r^2_{\overline{\nu}_e}\rangle < 7.3 \times 10^{-32} cm^2$

Table 4: *Limits on the neutrino charge radius squared obtained by accelerator and reactor experiments.*

Accelerator experiments		
$\mu_{\nu_e} < 1.08 \times 10^{-9}$	[57, 53]	$\nu_e e \to \nu_e e$
$\mu_{\nu_\mu} < 7.4 \times 10^{-10}$	[57, 53]	$\nu_\mu e \to \nu_\mu e$
$\mu_{\nu\tau} < 5.4 \times 10^{-7}$	[60]	$\nu_\tau e^- \to \nu_\tau e^-$
$\mu_{\nu\tau} < 4 \times 10^{-6}$	[62, 64]	$e^+e^- \to \nu\bar{\nu}\gamma$
Reactor experiments		
$\mu_{\nu_e} < 1.8 \times 10^{-10}$	[56]	$\bar{\nu}_e e \to \bar{\nu}_e e$
$\mu_{\nu_e} < 2.4 \times 10^{-10}$	[55]	$\bar{\nu}_e e \to \bar{\nu}_e e$
$\mu_{\nu_e} < 3 \times 10^{-10}$	[54, 45]	$\bar{\nu}_e e \to \bar{\nu}_e e$
Astrophysical Limits		
$\mu_\nu < (2\text{-}3) \times 10^{-12}$	[69, 70, 71, 74]	Luminosity of red giants
$\mu_\nu < 1 \times 10^{-11}$	[75, 76]	Cooling of helium stars
$\mu_\nu < (2\text{-}8) \times 10^{-12}$	[77]	Supernova 1987A
$\mu_\nu < (0.3\text{-}0.05) \times 10^{-12}$	[78]	Supernova 1987A
Cosmological Limits		
$\mu_\nu < (1\text{-}2) \times 10^{-11}$	[66]	^{4}He synthesis in the Big Bang
$d_\nu < 2.5 \times 10^{-22}$ e cm	[67]	^{4}He synthesis in the Big Bang

Table 5: *Upper bounds on dipole moments of the neutrino.*

4.2 Astrophysical Limits

4.2.1 Stellar Cooling

The existence of neutrino dipole moments could influence the rate of generation and emission of energy from a stellar plasma. In dense stars, an off-shell photon, plasmon, can couple to a dipole moment through $\gamma^* \to \nu_{m'}\bar{\nu}_m$. The produced neutrinos would escape with some energy E_ν, leading to a cooling of the core of the star. As the star in the main sequence burns hydrogen, the He^4 core increases, and so does the luminosity. When the core reaches a critical density the $3\alpha \to^{12} C + 7.27\ MeV$ ignites and the core size expands rapidly while the overall luminosity drops suddenly (helium flash). The dip is associated with neutrino losses. A large neutrino magnetic moment would delay helium ignition due to cooling from the reaction $\gamma^* \to \nu\bar{\nu}$ and the larger radius leads to a more efficient helium burning. The enhanced plasmon decay rate would lead to an increased core mass of $\frac{\Delta M_c}{M_\odot} = 0.013\frac{\mu_{\nu_e}}{10^{-12}\mu_B}$. The enhanced neutrino losses could accelerate the cooling rate of white dwarfs (WD). It was found that the "neutrino" dip at the bright side of the luminosity function was too deep unless $\mu_\nu < 10^{-11}\mu_B$. A comparison of luminosities of red giants in 26 globular clusters before and after helium flash sets the even smaller upper limit[69, 70, 71, 74]

$$\mu_\nu < (2-3) \times 10^{-12}\mu_B\ ,\quad CL = 90\%$$

These limits apply to both Majorana and Dirac neutrinos.

4.2.2 Supernova (SN1987A)

In the core of a collapsing star, neutrinos have an energy of $E_\nu \sim 100\ MeV$. The spin-flip reactions $\nu_L e^- \to \nu_R e^-$ and $\nu_L p \to \nu_R p$, induced by a hypothetical neutrino dipole moment, could produce sterile neutrinos (right handed Dirac neutrinos) that could escape freely, cooling the supernova and modifying the corresponding time scale. In addition, due to the the residual magnetic field of the interstellar medium, reflipping is possible, $\nu_R \to \nu_L$, and the lefthanded neutrinos could be detected on the earth by the Kamiokande and IMB detectors. The abscence of neutrinos with energies greater than 50 MeV in SN1987A and the study of the duration of the neutrino pulse lead to an upper limit of[77]

$$\mu_\nu < 10^{-12} - 10^{-13}\mu_B\ ,\quad CL = 90\%$$

The SN1987A bounds have recently been reexamined by Goyal et al.[78] by assuming the presence of a large number of pions and/or a very different composition of the core, consisting of degenerate quarks and leptons. They calculated the energy loss due to helicity flip scattering processes: $\pi^- p \to n + \nu_R\bar{\nu}_R(\nu_L\bar{\nu}_L)$, $\pi^-\nu_L(\bar{\nu}_R) \to \pi^-\nu_R(\bar{\nu}_L)$ and $q\nu_L(\bar{\nu}_R) \to q\nu_R(\bar{\nu}_L)$. They obtained the

limits

$$\mu_\nu < (0.3 - 0.05) \times 10^{-12} \mu_B \ , \quad CL = 90\%$$

by imposing bounds on the ν_R luminosity for the observed neutrino flux at Kamiokande II and IMB. The SN arguments however only apply to Dirac neutrinos, since for Majorana neutrinos $\nu_R = \overline{\nu}_R$ is not sterile.

4.2.3 ^4He-Nucleosynthesis

Using cosmological arguments, an upper limit to a possible magnetic moment of $\mu_\nu < (1-2) \times 10^{-11} \mu_B$ is obtained[66] by requiring that nucleosynthesis of ^{4}He in the Big Bang not be disrupted by the excitation of additional neutrino helicity states, through reactions like $e^\pm + \nu_R \leftrightarrow e^\pm + \nu_L$, $e^+e^- \rightarrow \nu_L \overline{\nu}_R, \nu_R \overline{\nu}_L$. The neutrino component would contribute with its full spin statistical weight of 2, rather than 1, as assumed in standard models of the Big Bang. The escaping sterile ν_R would then lead to a quicker cooling and hence to more He^4, of the order of 15%. The same arguments were used[67] to derive the only existing upper limit on neutrino electric dipole moments of

$$d_\nu < 2.5 \times 10^{-22} e \ cm \ , \quad CL = 90\%$$

Globular cluster limits quoted by Raffelt are $d_\nu < 2 \times 10^{-14} e \ cm$.

4.2.4 Radiative neutrino decays

Radiative decays of neutrinos $\nu_i \rightarrow \nu_j$ can proceed through transition dipole moments. The absence of a γ-burst in association with the SN1987A neutrino burst allows the lifetime of the neutrino to be constrained: $\frac{\tau_\nu}{m_\nu} \geq 2 \times 10^{15} s/eV$. The data stem from gamma ray observations by the Solar Maximum Mission Satellite[79]. Recently, new results are obtained by the COMPTEL instrument[72]. The results on τ_ν from SMMS can be expressed in terms of transition dipole moments

$$\frac{\mu_\nu}{\mu_B} \leq \left\{ \begin{array}{ll} 1 \times 10^{-8} \left(\frac{1eV}{m_\nu}\right) , & m_\nu \leq 20 \ eV \\ 5 \times 10^{-10} \left(\frac{1eV}{m_\nu}\right) , & m_\nu \geq 100 \ eV \end{array} \right\}$$

The stellar cooling arguments are valid up to neutrino masses of $\sim 10 \ keV$, whereas reactor experiments can go beyond. Upper limits from SN1987A are only valid for Dirac neutrinos, and those resulting from radiative neutrino decays depend on assumptions about the non-radiative decay modes. It is very unlikely that the upper bounds derived from astrophysics and cosmology can be improved by a factor of more than two[73]. Experiments, on the other hand, go by improvement steps of typically one order of magnitude. So it is very important to perform further laboratory measurements.

Before describing the MUNU project, we now address the question whether it is theoretically possible to generate large dipole moments with very small neutrino masses.

5 Are large μ_ν theoretically possible?

In the standard model, when right handed neutrinos are included, neutrinos can couple to the photon through higher order weak interactions Dirac neutrinos with mass m_ν acquire a magnetic moment[80],

$$\mu_\nu = \frac{3eG_F}{8\sqrt{2}\pi^2} m_\nu = 3.2 \times 10^{-19} \frac{m_\nu}{eV} \cdot \mu_B$$

where G_F is the Fermi coupling constant and $\mu_B = e/2m_e$ the Bohr Magneton.

$$m_{\nu_e} \simeq 10 \ eV \implies \mu_\nu^{SM} \simeq 3 \times 10^{-18} \mu_B$$

The simplest extension of the standard model is achieved by extending its gauge group structure. In the Left-Right symmetric models the group is $SU(2)_L \times SU(2)_R \times U(1)$ and new gauge

bosons, $W_R^{\pm}$ and Z_R are required. The mass of the neutrino in the SM expression above is replaced by a lepton mass times a certain mixing angle between the left- and right-handed gauge bosons:

$$\mu_\nu \simeq 3.2 \cdot 10^{-19} \frac{m_l \sin 2\theta}{eV} \cdot \mu_B$$

Relatively larger magnetic moments $\mu_\nu^{LR} \simeq 10^{-14}\mu_B$ could be reached[81].

Beyond Standard Model, Voloshin introduced a new ν-isospin symmetry based on the group $SU(2)_\nu$. The left-handed neutrino ν_L and the left-handed antineutrino $(\nu^c)_L$, defined as the antiparticle of the right-handed neutrino, form a doublet[82]

$$\begin{pmatrix} \nu \\ \nu_L^c \end{pmatrix} \; ; \; \begin{pmatrix} \eta_1^+ \\ \eta_2^+ \end{pmatrix} \; ; \; \tau^-$$

the τ (for illustration) is a singlet of ν-isospin. It happens that the $SU(2)_\nu$ symmetry permits magnetic moments while prohibiting masses, as discussed in Ref.[86]. A Dirac neutrino mass term, of the form $\frac{M_D}{2}\left(\nu^{cT}C\nu + \nu^T C\nu^c\right)$ has the ν-spin structure $(\downarrow\uparrow + \uparrow\downarrow)$. It is a component of a ν-spin triplet that is not invariant under rotations in ν-spin space, and consequently is forbidden. The same arguments hold for a Majorana mass term. The dipole moment interaction $\mu_\nu \overline{\nu}\sigma_{\alpha\beta}\nu F^{\alpha\beta}$, which can be written as $\frac{\mu_\nu}{2}\left(\nu^{cT}C\sigma_{\alpha\beta}\nu - \nu^T C\sigma_{\alpha\beta}\nu^c F^{\alpha\beta}\right)$, has the ν-spin structure $(\downarrow\uparrow - \uparrow\downarrow)$, which is a singlet invariant under ν-spin rotations, and consequently is allowed.

In addition to the $SU(2)_L$ symmetry of the standard model, a new symmetry is introduced[84], the horizontal symmetry $SU(2)_H$, which connects the usual e- and μ-generations

$$\begin{pmatrix} \nu_e & \nu^\mu \\ e & \mu \end{pmatrix}_L \; ; \; \begin{pmatrix} \nu_\tau \\ \tau \end{pmatrix}_L \; ; \; \begin{pmatrix} \eta_1^+ & \eta_2^+ \end{pmatrix}_L$$

A horizontal doublet of Higgs scalars is required and neutrinos are Majorana particles. This model predicts relatively large magnetic moments while masses are kept small. It has been shown ([83]) that a bound on the Higgs mass of $M_H < 100\ GeV$ can be obtained for $m_\nu < 10\ MeV$ and $\mu_\nu \sim 10^{-11}\mu_B$. Other models incorporating large dipole moments are described in references [94, 87].

6 The MUNU Detector at the Bugey Reactor

Antineutrino electron scattering at very low energies will be measured by the MUNU collaboration to probe μ_ν[88, 89, 90, 91, 92].

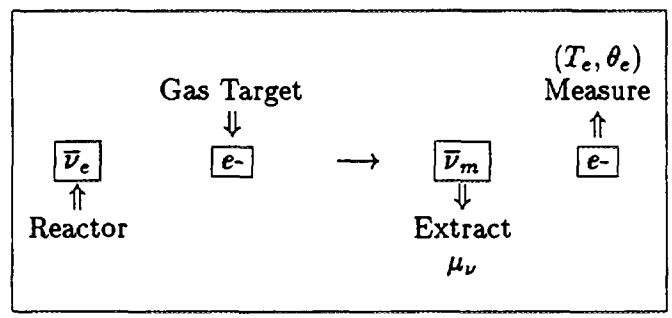

The Requirements are

- (High Flux + Low Energy) $\overline{\nu}_e$	$\Longrightarrow$	⋆ REACTOR
- Measure Track (Energy + Angle)	$\Longrightarrow$	⋆ TPC
- Minimise $\overline{\nu_e}p \to e^+n$	$\Longrightarrow$	⋆ no Hydrogen
- Very low Background	$\Longrightarrow$	⋆ radiochemically clean materials
		⋆ Anti-Compton
		⋆ Shielding

MUNU chose the Bugey nuclear reactor, a Time Projection Chamber filled with CF_4-Gas, a mineral oil based liquid scintillator as anti-compton, readout with photomultipliers, and lead and polyethylene as shielding.

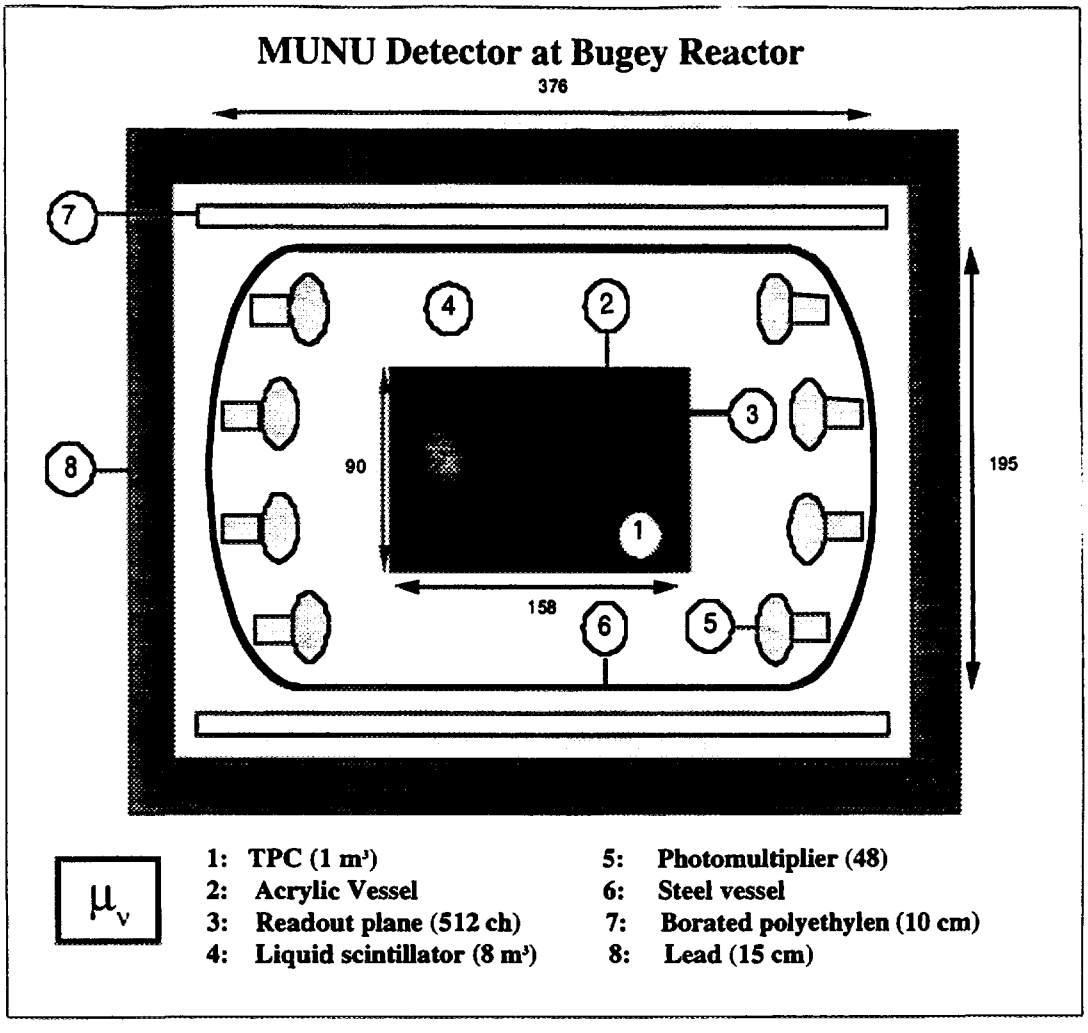

Figure 12: *The MUNU detector at Bugey reactor.*

The Bugey 5 reactor has a power of 2800 $MWth$ and produces $5 \times 10^{20}\ \overline{\nu}_e/s$ in 4π. It is located about 40 km east of Lyon and 150 km from Geneva. The detector will be installed 18.6 m from the core (20 m water equivalent), where the antineutrino flux is $\sim 10^{13}\overline{\nu}_e/s \cdot cm^2$. The cosmic muon flux is $\sim 32/s \cdot m^2$.

A schematic view of the detector is shown in Fig.12.

The Time Projection Chamber (TPC)

The container is a cylindrical acrylic vessel of length 158 cm and diameter 90 cm. The CF_4 gas is chosen as target and detector because of the following properties:

- It has a low Z (C=6, F=9), which minimises multiple scattering,
- a high electron density of 3.68 g/l, corresponding to 6 10^{27} e/m^3 at 5 bar, and
- a high drift velocity of 4 cm/μ for 600 V/cm at 5 bar.
- CF_4 is not toxic, not flammable and relatively cheap (2 CHF/l).
- It is a pure electron target (no free Hydrogen), which suppresses the reaction $\overline{\nu_e}p \rightarrow e^+n$.

Details of the TPC (no magnetic field!) are given in Fig.13. The cathode (negative high voltage) is on the top and the readout plane on the bottom. The anode wires are connected together to provide a total energy trigger signal. A threshold of 500 keV is forseen at the beginning. Two planes of 256 perpendicular strips (3.3 mm pitch) pick up induced signals and define the x, y coordinates. The z coordinate is obtained through the time evolution of the signal. The anode and strip signals are sampled by a 25 MHz- flash ADC system. The spatial resolution is $\sigma_{x,y,z} \sim 1\ mm$. From the first 2 cm of the track it is possible to determine the angle of the recoil

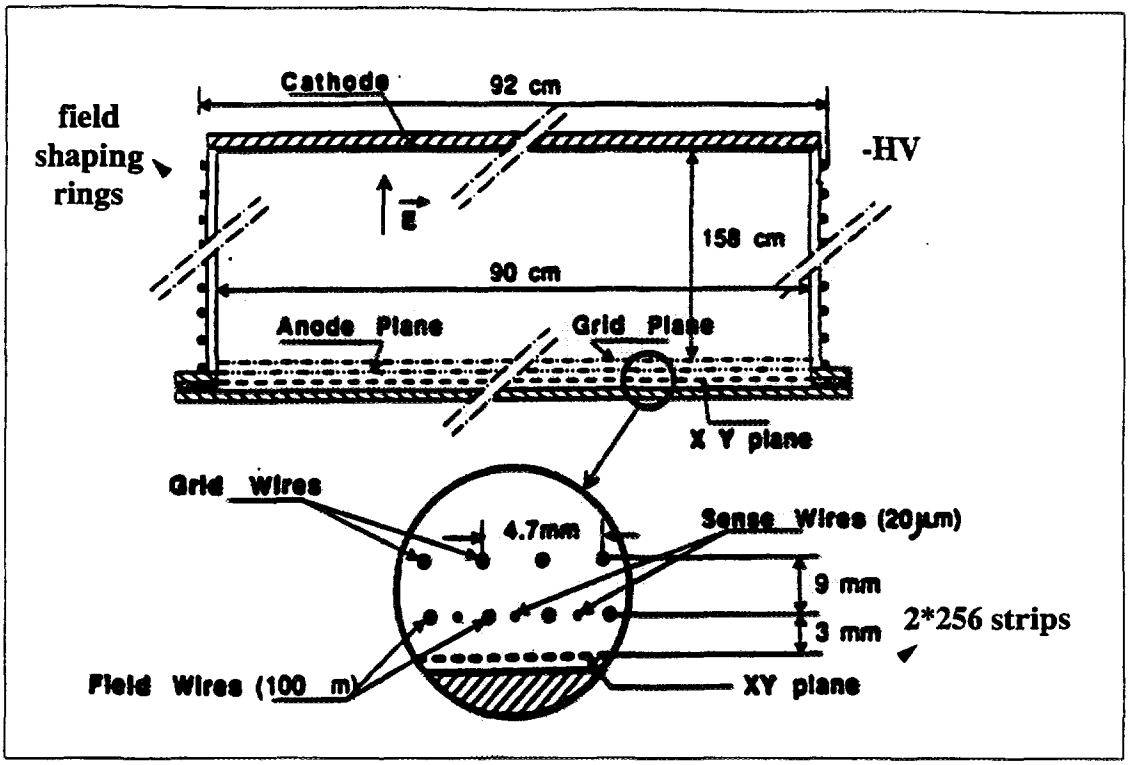

Figure 13: *MUNU Time Projection Chamber*

electron, θ_e, with an accuracy of $\sigma_\theta \sim 15°$. This is mainly due to multiple scattering. The core size of the reactor contributes to $\pm 6°$.

Tests with a prototype mini TPC ($\Phi = 10\ cm, L = 30\ cm$) have been concluded, and electron and muon tracks are seen (Fig.14). Preliminary results have also been obtained with a full scale ($1\ m^3$) TPC. Fig.15 shows a muon event. The signal to noise ratio is about 10 to 1.

The Liquid Scintillator and the shielding

Eight m^3 mineral oil based liquid scintillator (NE235, attenuation length $\lambda_{att} \sim 6.5\ m$ at $420\ nm$) are contained in a stainless steel vessel supporting 5 bar ($L = 376\ cm$, $\Phi = 195\ cm$). It acts as an anti-Compton shield and allows detection of low energy photons and vetos cosmic muons. It is readout by 48 photomultipliers (EMI9351 8", B53 glass with 0.2 Bq; 100 keV threshold; 180 photoelectrons/MeV; FADC readout). The passive shielding is based on 15 cm low activity lead to reduce local activity and 10 cm borated polyethylene (CH_2+B_4C) to reduce the neutron flux created in lead by cosmic muons.

Background Studies and sensitivity

Background, defined to be γ and β rays giving one single electron in the chamber, depositing less than 100 keV in the Anti-Compton shield and at least 500 keV in the TPC, comes from three sources.

Natural activities : (Th, U, K, ^{60}Co, etc...)
All materials must be radiochemically clean, especially the ones present in large quantities. For example, mineral oil and acrylic are produced with concentrations of Th and U of $< 10^{-12}$g/g. One expects 1.5 evts/day.

Muons:
Muons can be captured either in the TPC: $\mu + {}^{12}C({}^{19}F) \rightarrow {}^{12}B({}^{19}O) + \nu$, followed by the decay of ${}^{12}B({}^{19}O)$ with neutron emission (0.5 evts/day), or can interact in the shielding (0.6 evt/day).

Neutrons:
Slow neutrons from the reactor lead to a negligible background. Those induced by muons contribute to 0.15 evt/day, and those from $\overline{\nu_e} p \rightarrow e^+ n$ in the scintillator to 0.15 evt/day.

From measurements, simulations and the experience gained with the Xe-TPC at Gotthard, $\sim$ 3 background events are expected per day[88]. The trigger is based on 3 levels, corresponding to the following photon energy levels

- $E > 100\ keV \Longrightarrow \gamma$ rejection (100 Hz, 40 μs)

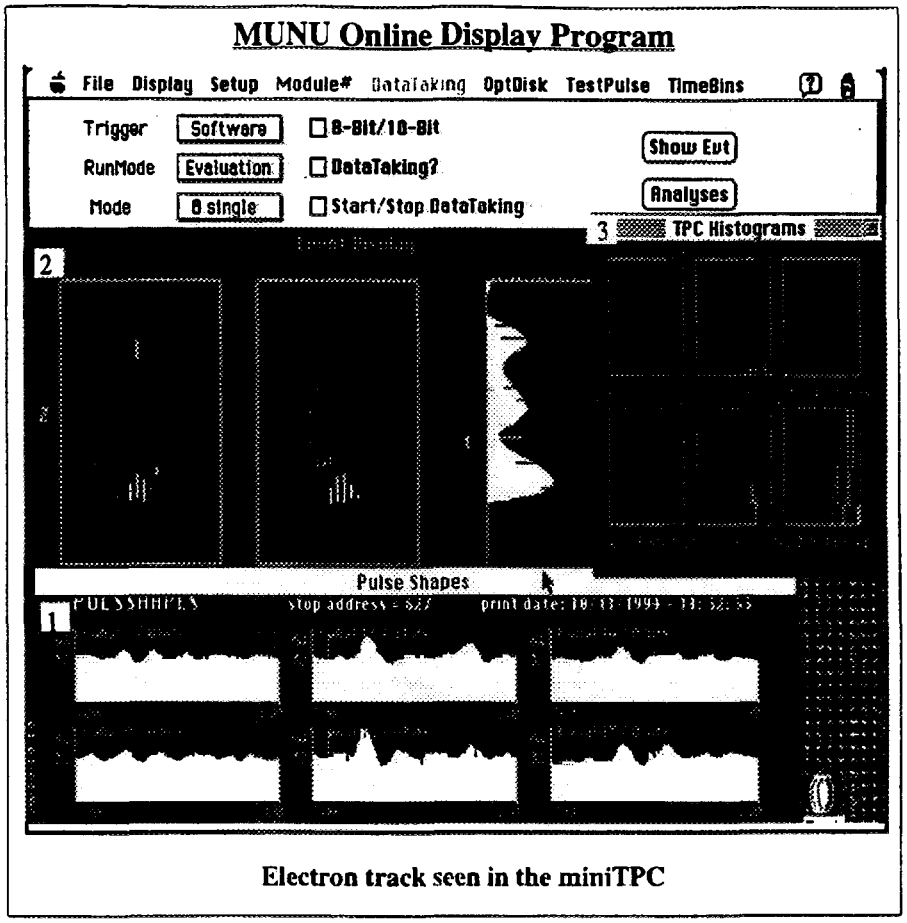

Figure 14: *Electron track seen in the mini TPC.*

- $E > 1.0\ MeV \Longrightarrow \beta$ rejection (50 Hz, 200 μs)
- $E > 5.0\ MeV \Longrightarrow \mu$ rejection (400 Hz, 200 μs)

The expected event rate and the corresponding detector acceptance are summarised in Tab.6 for two energy domains, $0.5 - 1.0\ MeV$ and above $1.0\ MeV$. A hypothetical magnetic moment of 10^{-10} would increase the event rate by $\sim 30\%$.

		$\bar{\nu}_e$ events/day (**year**)	
T[MeV]	Acceptance	$\mu_\nu = 0$	$\mu_\nu = 10^{-10}$
0.5-1.0	0.85	5.3	8.0
		1530	**2400**
≥ 1	0.65	4.2	5.3
		1230	**1560**
σ		9.5	13.4
		Background ~ 3 events/day	

Table 6: *Expected Event Rates[88]*

The MUNU detector presents new features. The energy domain $E_\nu = 0.5 - 1.5\ MeV$ has so far not been explored. The scattering angle θ_e will be measured. As a consequence, background can be measured while reactor is on, by considering events in the backward hemisphere ($\theta_e > 90°$). The data taking will spread over at least one year, giving 5 times more events above $1.5\ MeV$ than observed at Savannah.

Assuming 1 year of data taking and considering only the low energy domain ($0.5 - 1.0\ MeV$), one expects $\pm 3\%$ statistical errors. Systematic uncertainties ($\pm 5\%$) are mainly due to the reactor spectrum ($\pm 3\%$), the reactor power ($\pm 2\%$), and the detection efficiency ($\pm 3\%$).

With a background of about 3 events/day one obtains a sensitivity of

$$\mu_\nu < 3 \times 10^{-11} \mu_B\ ,\quad CL = 90\%$$

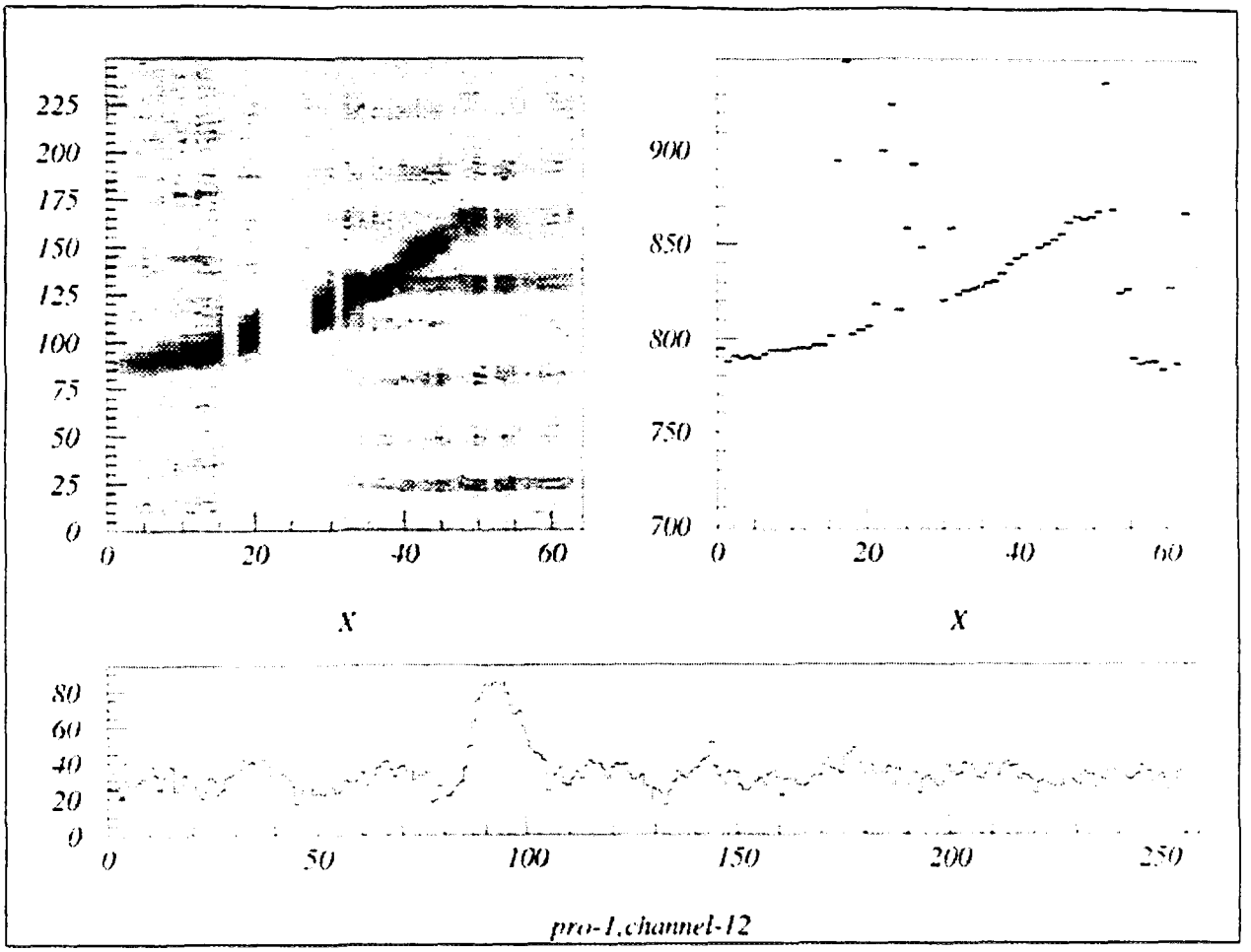

Figure 15: *Muon event seen in a full scale TPC.*

decreasing to $\mu_\nu < 4 \times 10^{-11}\mu_B$, if the background is 4× higher than anticipated. The sensitivity could be improved to

$$\mu_\nu < 2 \times 10^{-11}\mu_B \ , \quad CL = 90\%$$

by considering the following. The use of the energy bin above 1 MeV allows the slope of the reactor spectrum to be extracted, and hence, the systematic uncertainties to be reduced. The angular distribution will be measured. Depending on the background situation the threshold could be lowered to $300 - 350$ keV, and the pressure to 2-3 bar.

On the other hand, assuming a vanishing magnetic moment, the weak mixing angle can be measured, in $\overline{\nu_e}e^-$-scattering at very low energies, with an accuracy

$$\Delta \sin^2 \theta_W = \pm 5\%$$

comparable to that achieved by the CHARM II collaboration in the study of $\nu_\mu e$-scattering[95, 58]

All components of the MUNU detector are ready and tested. Data taking is expected to start by the beginning of 1997. Various features of the detector, like tracking and low background, make MUNU a general multipurpose low energy detector. It can be used to look for double beta decay (see J. Busto, these proceedings) or dark matter[88]. Simulations are being performed to study the feasability of a Super Solar MUNU (SSM), to detect solar neutrinos.

7 Summary and Prospects

To summarise, the neutrino is very important for particle physics, astrophysics and cosmology. It is necessary to study all its properties independently... including its possible electromagnetic interactions.

Several complementary upper limits on neutrino dipole moments and charge radius have been obtained by laboratory experiments at reactors and accelerators, or by using astrophysical arguments. The latter are more stringent but more or less model dependent. It is important to perform more direct measurements, and new experiments, like MUNU, are welcome.

8 Acknoweledgements

I would like to thank the organizers of the Zuoz school, especially Milan Locher, for the warm hospitality and for a pleasant stay in a wonderful place.

References

[1] F. Reines, C.L. Cowan, *Phys. Rev.*, **90**(1953) 492.

[2] C.L. Cowan, H.W. Cruse, F.B. Harrison, A.D. McGuire, F. Reines, *Science*, **124**(1956) 103

[3] M. Goldhaber, L. Grodzins, A.W. Sunyar, *Phys. Rev.*, **109**(1958) 1015.

[4] G. Danby, J.M. Gaillard, K Goulianos, L.M. Lederman, M. Mistry, M. Schwartz, J. Steinberger, *Phys. Rev. Lett.*, **9**(1962) 36.

[5] M.L. Perl et al., *Phys. Rev. Lett*, **35**(1975) 1489.

[6] Belesev et al., Phys. Lett.**B350**(1995)263.

[7] Assamagan et al., Phys.Rev.**D53**(1996)6065.

[8] Buskulic et al., Aleph coll., Phys. Lett.**B349**(1995)585.

[9] G. Barbiellini, G. Gocconi, Nature **329** (1987)21.

[10] E. Majorana, Nuovo Cimento **14** (1937) 171.

[11] F. Boehm and P. Vogel, Physics of Massive Neutrinos (Cambridge University Press, 1987/1992)

[12] B. Kayser, Comments Nucl. Part. Phys.**14**(1985)69

[13] J.N. Bahcall, M.H. Pinsonneault, Rev. Mod. Phys.**64**(1992)82.

[14] S. Turck-Chièze, I. LopesRev. Mod. Phys.**64**(1992)82.

[15] B.T. Cleveland et al., Nucl. Phys. (Proc. Supp.)**B38**(1995)47; B.T. Cleveland et al., subm. to Astrophys. J.(1996).

[16] P. Anselmann et al., Phys. Lett.**B357**(1995)237.

[17] J.N. Abdurashitov et al., Nucl. Phys. (Proc. Supp.)**B38**(1995)60.

[18] "Solar neutrino data from Kamiokande" Y. Suzuki et al., Nucl. Phys. (Proc. Supp.)**B54**(1995)47.

[19] R, Davis, in Proc. 7th Work. on Grand Unif., ICONABAN'86, ed. R. Arafune (Singapore: World Scientific)273.

[20] J.N. Bahcall, "Neutrino Astrophysics.", Cambridge University Press, 1989

[21] M.B. Voloshin, M.I. Vytsotskii and L.B. Okun, Sov. Phys. JETP**64**(1986)446.

[22] W. Hampel, these proceedings.

[23] A. Dar, these proceedings.

[24] S. Petcov, these proceedings.

[25] D.S. Oakley et al., Astrophys. J.(1994) **437**,L63

[26] R. L. McNutt Jr, Science **270**(1995)1635

[27] D.S. Oakley, H.B. Snodgrass,hep-ph/9604252, 1996

[28] L. Wolfenstein, Phys. Rev. D17 (1978) 2369; Phys. Rev. D20 (1979) 2634

[29] S.P. Mikheyev, A.Yu. Smirnov, Sov. J. Nucl. Phys. 42 (1986) 913; Sov. Phys. JETP 64 (1986) 4; Nuovo Cimento 9C (1986) 17.

[30] C.S. Lim, W.J. Marciano Phys. Rev. D37 (1988)1368.

[31] W.J. Marciano, A. Sirlin, Electromagnetic properties of neutrinos, Brookhaven,1988.

[32] E. Akhmedov and M. Khlopov, Mod. Phys. Lett. **A3** (1988) 451.

[33] E. Akhmedov and M. Khlopov,

[34] E. Akhmedov Nucl. Phys. **A527** (1991)679.

[35] E. Akhmedov, A. Lanza and S. Petcov, Phys. Lett. **B303** (1992)85

[36] J. Pulido, Phys. Rev.**D48** (1993)1492.

[37] H.Nunokawa, H. MinakataPhys. Lett.**B314** (1993)371

[38] E. Akhmedov, FTUV**94-26** (1994)

[39] C.S. Lim, H.Nunokawa, Astropart. Phys.**4** (1995)63.

[40] W. Pauli, Phys. Today **23** (sept 1978).

[41] P.B. Pal, Inter. J. of Mod. Phys. **A7** (1992) 5387.

[42] J. Pulido, Phys. Rep. **211** (1992) 167.

[43] G. Domogatskii,D. Nadezhin, Sov. J. Nucl. Phys.**12**(1971)678

[44] A.V. Kyuldjiev, Nucl. Phys.**B243**(1984)387

[45] P. Vogel und J. Engel, Phys. Rev. D,**39**(1989)3378

[46] J. Segura, J. Bernabeu, F.J. Botella, J. Penarrocha, Phys. Rev. D49 (1994)1633.

[47] J. Segura, Tesis Doctoral, Universidad de Valecia, Noveiembre 1994,,

[48] J. Bernabeu, S.M. Bilenky, F.J. Botella, J. Segura, Nucl. Phys. B426 (1994)434.

[49] G. DeGrassi, A. Stirlin, W.J. Marciano, Phys. Rev.**D39**(1989)287.

[50] K. Abe et al., Phys. Rev. Lett. **58**(1987)636;

[51] J. Dorenbosch et al., Z. Phys**41**(1989)567.

[52] Ahrens et al., Phys. Rev.**D41**(1990)3297.

[53] Allen et al., Phys. Rev.**D47**(1993)11.

[54] F. Reines, H.S. Gurr and W. Sobel, Phys. Rev. Lett.,**37**(1976)315

[55] G.S. Vidyakin et al., JETP Lett. **49** (1989) 740; G.S. Vidyakin et al., JETP Lett. **55** (1992) 206.

[56] Derbin et al., JETP Lett. **57** (1993) 768(translated from ZETFP **57** 755); Derbin et al., PAN **57** (1994) 222 (transl. from YAF **57** 236)

[57] D.A. Krakauer et al., Phys. Lett.**252B**(1990)177; Phys. Rev.,**44D**(1991)6.

[58] CHARM II collab., P. Vilain et al., Phys. Lett.**B345**(1995)115.

[59] CHARM collab., Dorenbosch et al., Z. Phys.C41(1989)567; Z. Phys.C51(1991)142.

[60] A.M. Cooper-Sarkar et al., Phys. Lett.B280(1992)153.

[61] H. Grässler et al., Nucl. Phys.**B273**(1986)1253.

[62] H. Grotch, R. Robinet, Z. Phys.C39(1988)553.

[63] T.M. Gould, I.Z. Rothstein, Phys. Lett.B333(1994)545.

[64] M. Acciarri et al., Phys. Lett.B346(1995)190.

[65] G. G. Raffelt, Phys. Rep. 198 (1990) 1-113.

[66] J.A. Morgan, Phys. Lett. B102 (1981) 247.

[67] "Upper limit on neutrino electric dipole moments."
J.A. Morgan, D.B. Farrant, Phys. Lett. 128B (1983) 431.

[68] G. Raffelt and D. Dearborn, Phys. Rev. D37 (1988) 549.

[69] G. Raffelt, Phys. Rev. Lett. **64** (1990) 2856.

[70] G. Raffelt, Astrophys. J. 365 (1990)559;

[71] G. Raffelt, A. WeissAstron. Astrophys. 264 (1992)536;

[72] G. G. Raffelt, these proceedings.

[73] G. G. Raffelt, private communication.

[74] M. Catelan et al., Astrophys. J. 461 (1996)231;

[75] G. Raffelt, D. Deaborn, Silk, A. Phys. J. 336 (1989)61.

[76] M. Fukugita, S. Yazaki, Phys. Rev. D36 (1987)3817.

[77] J. M. Lattimer, J. Cooperstein, Phys. Rev. Lett. **61**(1988)23; R. Barbieri, R.N. Mohapatra, Phys. Rev. Lett. **61**(1988)27; I. Goldman et al., Phys. Rev. Lett. **60** (1988) 1789; D. Notzold, Phys. Rev. **D38** (1988) 1658.

[78] A. Goyal, S. Dutta, S.R. Choudhury, Phys. Lett. **B346**(1995)312.

[79] L. Oberauer, Asttropart. Phys. **1**(1993)377; E.L. Chupp et al., Phys. Rev. Lett. **62**(1989)505.

[80] B.W. Lee, R.E. Schrock, Phys. Rev. **D16**(1976)1444; W. Marciano, A.I. Sandra,Phys. Lett.**B67**(1977)303.

[81] M. Baig, J.A. Grifols, E. Masso, Mod. Phys. Lett. **A3**(1988)719

[82] M.B. Voloshin, Sov. J. Nucl. Phys. **481**(1988)225; R. Barbieri, R.N. Mohapatra, Phys. Lett. **218B**(1989)1225; K.S. Babu, R.N. Mohapatra, Phys. Rev. Lett. **63**(1989)228

[83] M. Leurer, N. Marcus, Phys. Lett.**B237**(1990)81.

[84] K.S. Babu, R.N. Mohapatra, Phys. Rev. Lett. **64**(1989)1705

[85] S.M. Barr, E.M. Freire, A. Zee, Phys. Rev. Lett. **65**(1990)2626

[86] B. Kayser, Nucl. Phys. B (proc. suppl.)**19**(1991)177.

[87] M. Voloshin, Nucl. Phys. B (proc. suppl.)**19**(1991)433.

[88] MUNU Collaboration: Grenoble, Münster, Neuchatel, Padova, Zürich, C. Broggini et al., Proposal, LNGS 92-47 (1992) 51 pp.

[89] C. Amsler (MUNU Collab.), Proc. of the 3rd NESTOR Workshop, Pylos, Greece (1993)556.

[90] C. Broggini (MUNU Collab.), Nucl. Phys. B (proc. suppl.)**35**(1994)441.

[91] J. Busto (MUNU Collab.), Proc. XXII Int. Conf. on High Energy Physics, 20-27 July 1994, Glasgow, p.955.

[92] M. Avenier et al. (MUNU Collab.),Contribution to the XVI Conf. of Neutrino Physics and Astrophysics, Eilat, 1994; INSNG 94/56.

[93] R. N. Mohapatra und P. B. Pal, Massive Neutrinos in Physics and Astrophysics (World Scientific, Singapore 1991)

[94] P. B. Pal, University of Oregon, Institute of Theoretical Science, OITS **470** (1991)

[95] D. Geigerat et al., Phys. Lett. **B259**(1991)499.

[96] Particle Data Group, Physical Review **D54/1-I** (The American Physical Society, 1996)1